Chapter 2
Chlorophyll-Based Generators of Proton Potential

Generators of $\Delta\bar{\mu}_{H^+}$ play a leading role in the conversion of external energy sources into forms that can be used by living cells. We begin by discussing light-dependent (photosynthetic) generators. First of all, we consider them to have been the primordial systems for proton potential generation driven by external energy sources during the evolution of life. Second, photosynthesis still plays the key role in energy supply to the biosphere. The biosphere is known to consist mainly of photosynthetic organisms and organotrophs that directly or indirectly consume products of photosynthesis—organic substances and oxygen. Oxygenic photosynthesis, i.e. photosynthesis that produces oxygen, takes place in green plants and cyanobacteria. It is this type of photosynthesis that provides oxygen for the planet. One can point to the precise geographic coordinates of the areas of the Earth that are responsible for this function. Most of the Earth's oxygen is produced in the taiga forests in Siberia. Canada, with its temperate zone forests, especially coniferous ones, provides a smaller contribution. The famous tropical forests (African and South American jungles) as well as the World's ocean do not play an important role in this process due to the presence of vast numbers of heterotrophic bacteria that absorb that very oxygen that is produced by photosynthetic organisms. So, Siberia can be compared to the planet's lungs, and if Siberian forests are destroyed it will mean the end of aerobic life on Earth.

There is one other technical but nevertheless important point that explains our decision to start our presentation with photosynthesis. This process is initiated by a quantum of light, and this fact makes it possible to use modern physical instrumentation for the analysis of its mechanism. For instance, when using an ultrafast laser one can generate a 2×10^{-14} s long flash of light so as to study kinetics and mechanisms of the primary processes of light energy storage.

V. P. Skulachev et al., *Principles of Bioenergetics*,
DOI: 10.1007/978-3-642-33430-6_2, © Springer-Verlag Berlin Heidelberg 2013

2.1 Light-Dependent Cyclic Redox Chain of Purple Bacteria

Let us start not from that main (oxygenic) photosynthesis that has just been mentioned above, but from the more primitive photosynthetic mechanisms that have been described in phototrophic bacteria (they have already been mentioned in the Chap. 1). The photosynthetic apparatus of purple bacteria is located in the internal (i.e. cytoplasmic) membrane and in chromatophores—intracellular vesicles that split off that membrane.

The biological membrane is composed of lipids and proteins. It is essentially a lipid bilayer with transmembrane proteins floating in it. There are also other proteins that are attached to the surface of the bilayer. Biomembranes usually contain more protein than lipid, even though there are some where lipid prevails. Usually it is phospholipids that form the lipid component of biomembranes, but sometimes this function is fulfilled by sulfolipids or glycolipids.

One of the varieties of chlorophyll—bacteriochlorophyll—plays the key role in photosynthesis in the purple bacteria (see structure in Appendix 2). In the second half of the 1940s, Alexander Krasnovsky (Fig. 2.1) discovered reactions of photoinduced chlorophyll oxidation and reduction (Krasnovsky 1948), this discovery being the first step in the understanding of the mechanism of functioning of the photosynthetic apparatus.

Absorption of visible light by a chromophore molecule is known to induce transfer of an electron from the main orbital (S_0) to one of the singlet (S_1^*, S_2^* …) or triplet (T) excited orbitals (Fig. 2.2). Photon energy is spent during this process to transfer of the electron to an orbital that is further away from the nucleus. When in the excited orbital, the electron has a relatively weak connection to the nucleus, and thus it can be easily torn away from the chromophore molecule. So, this molecule in an excited state becomes a good *reductant*. Absorption of a light quantum produces at the same time a "vacancy" for an electron in the main orbital ("a hole"). This "hole" has substantial affinity for an electron, i.e. it is a good *oxidant*.

The lifetime of a chromophore molecule in an excited state (especially in a singlet state) is extremely short. The electron is inclined to return from an excited

Fig. 2.1 Alexander Krasnovsky

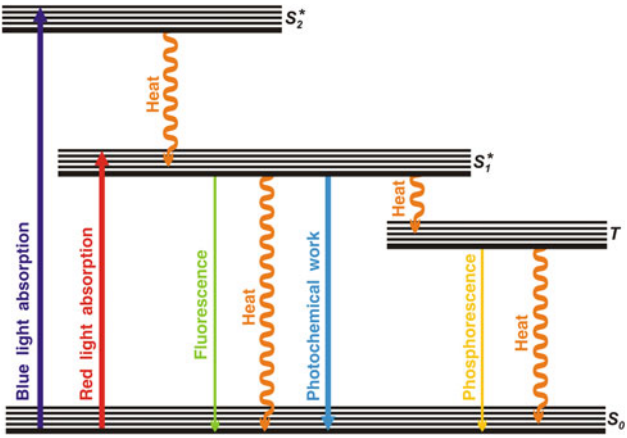

Fig. 2.2 Scheme of electron transfer induced by photon absorption by a chromophore

to the main orbital. Such a return is accompanied with dissipation of the absorbed photon energy in the form of heat or in the form of a light of longer wavelength (fluorescence or phosphorescence). But photosynthesizing organisms have learned to use the effect of chromophore transition into an excited state for the storage of the energy of the quantum (*hv*) in a form which is useful for a cell. For instance, if during the excited state lifetime an electron is transferred from the excited orbital to some acceptor X, and the vacancy on the main chromophore orbital is filled from some donor Y, then part of the energy of the photon can be stored as a difference of redox potentials of substances X and Y under the condition that the redox potential of the $Y_{oxidized}/Y_{reduced}$ couple is more positive than that of the $X_{oxidized}/X_{reduced}$ couple. Even more so, if this redox reaction is organized in such a way that an electron is transferred from Y to X *across* the membrane, then a certain part of the energy of the light quantum can also be stored as $\Delta\bar{\mu}_{H^+}$. Just in this way the most important photosynthetic process, i.e. oxygenic photosynthesis, is organized.

In an alternative and simplified version of photosynthesis, an electron from an excited orbital is returned to the main orbital, but not directly. It has to cross the membrane first, which leads to generation of $\Delta\bar{\mu}_{H^+}$. This type of photosynthesis is found in purple bacteria.

2.1.1 Main Components of Redox Chain and Principle of Their Functioning

Light is absorbed by a magnesium porphyrin moiety of bacteriochlorophyll, which is bound to a special protein (the *light-harvesting antenna complex*) or by additional pigments—*carotenoids*—located in the same membrane and transferring the

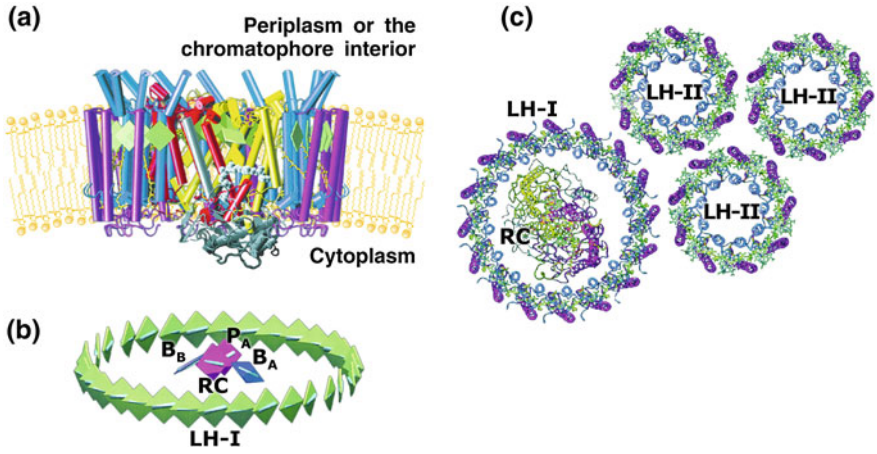

Fig. 2.3 **a**, **b** Structure of the reaction center complex (RC) and of antenna I (LH-I) of purple bacteria. Bacteriochlorophylls are represented as rhombs. Bacteriochlorophylls of antenna I are shown in green color; $(BChl)_2$ (it is labeled P_A); and bacteriochlorophyll monomers (B_A and B_B) of the reaction center are *red* and *blue*, respectively. The α-helical columns of the reaction center subunits are presented as colored *rods—yellow* (*L*-subunit), red (*M*-subunit), and *gray* (*H*-subunit). Antenna I proteins are shown as *blue* and *pink rods*. Bacteriopheophytins are not shown. **c** Structural arrangement of the reaction center complex, antenna I, and antenna II in purple bacteria. The polypeptide chain of the proteins and bacteriochlorophyll molecules are shown. (Hu et al. 1998)

excitation energy to the antenna bacteriochlorophyll. One should note that in the case of acidophilic bacteria Mg^{2+} ions are replaced by Zn^{2+} ions in bacteriochlorophyll, so that the Mg^{2+} of the porphyrin complex would not be replaced by H^+ ions, which would otherwise occur under acidic conditions (Wakao et al. 1996). The excitation migrates through antenna bacteriochlorophyll until it reaches what is called a "special pair", a *bacteriochlorophyll dimer* bound to other proteins forming a *photosynthetic reaction center complex* (Fig. 2.3).

Besides the dimer, the complex contains two *bacteriochlorophyll monomers*, two *bacteriopheophytins* (i.e. bacteriochlorophyll analogs where the Mg^{2+} ion is replaced by two H^+ ions), and two ubiquinone molecules (CoQ).[1] The amount of reaction center pigment complex is usually about two orders of magnitude smaller than that of the antenna pigment complex.

The excited bacteriochlorophyll dimer serves as an electron donor to ubiquinone (CoQ). This process is directed across the membrane to its cytoplasmic side. It includes a number of intermediate stages with consecutive reduction and oxidation of bacteriochlorophyll monomer, bacteriopheophytin, and bound MQ and/or CoQ (reactions 1–4 in the scheme of the cyclic redox chain, Fig. 2.4).

[1] In certain bacteria, one of the ubiquinone molecules is replaced by a menaquinone (MQ); see structure in Appendix 2.

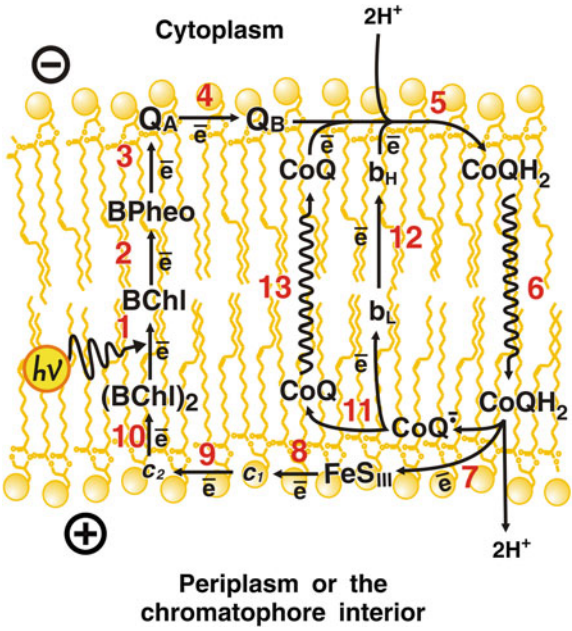

Fig. 2.4 Cyclic redox chain of the purple photosynthetic bacterium *Rhodospirillum rubrum*: $(BChl)_2$ and BChl—dimer and monomer of reaction center bacteriochlorophylls; BPheo—bacteriopheophytin; Q_A and Q_B—two ubiquinone molecules bound to reaction center proteins; b_H and b_L—high- and low-potential hemes of ; FeS_{III}—nonheme iron protein; c_1 and c_2—respective cytochromes (Skulachev 1988)

For reduction, CoQ needs two electrons and two protons (Fig. 2.5). One of these electrons is donated by the reaction center and the other by heme b_H of cytochrome *b*.[2] Having accepted two electrons, CoQ combines with two protons from the nearest water phase (above the membrane, i.e. in the cytosol in Fig. 2.4; $CoQH_2$ formation is described by reaction 5 in Fig. 2.4 and in more detail in Fig. 2.5).

When formed, $CoQH_2$ diffuses across the membrane in the direction of its opposite (periplasmic) side (Fig. 2.4, reaction 6). Close to this membrane surface, $CoQH_2$ is oxidized to the semiquinone form (reaction7) by the *nonheme iron–sulfur (FeS) protein* abbreviated as FeS_{III}. When $CoQH_2$ is oxidized, two H^+ ions are released to the periplasm or inside the chromatophore (Fig. 2.4).

The electron accepted by FeS_{III} is later used for the reduction of the bacteriochlorophyll dimer that was previously oxidized during the first stage of the cycle. Cytochromes of *c* type participate in the electron transfer from FeS_{III} to $(BChl)_2^{\bullet+}$ (reactions 8–10; in the case of *Rhodospirillum rubrum* these are cytochromes c_1 and c_2).

The radical ion $CoQ^{\bullet-}$ that appears after $CoQH_2$ has lost one electron and two protons reduces heme b_L (reaction 11). The latter transfers the electron to the

[2] Cytochromes are heme-containing proteins catalyzing redox processes (for heme structures, see Appendix 2). Cytochromes having the same heme group and differing in the protein moiety are usually indicated by the same letter but different numerical indexes.

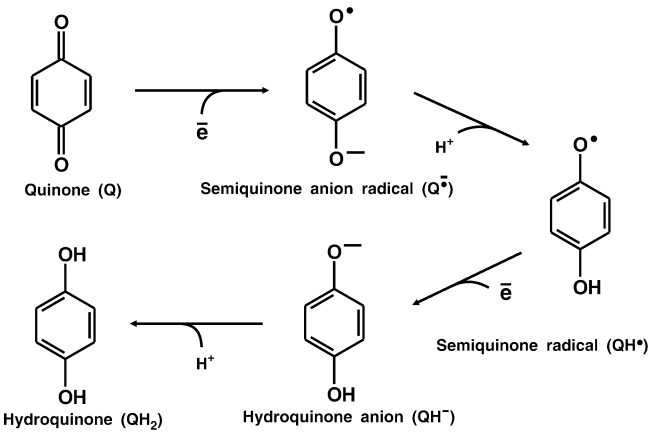

Fig. 2.5 Steps of conversion of quinone to hydroquinone (quinol) (Rich 1984)

previously oxidized heme b_H (reaction 12). The cycle is completed by diffusion of the formed CoQ to the cytoplasmic surface of the membrane (reaction 13).

The net result of the entire cycle is $\Delta\bar{\mu}_{H^+}$ *generation due to the transmembrane uphill transport of two* H^+ *ions per photon absorbed by BChl*.

The energy for the cycle is provided by photoexcitation of bacteriochlorophyll. The latter, being excited by a photon, greatly changes its redox potential, which becomes about −950 mV instead of +440 mV in the nonexcited state. All the further electron transfers go energetically downhill, i.e. from negative to more positive redox potentials (Fig. 2.6a).

The proteins catalyzing the cyclic electron transfer can be separated into two distinct complexes—the reaction center complex and the bc_1 complex.

2.1.2 Reaction Center Complex

Protein Composition. The reaction center complex isolated from *Rhodospirillum rubrum* is formed by *three protein subunits*—the so-called heavy (H), medium (M), and light (L) subunits. The subunit stoichiometry in the complex is 1:1:1 (Okamura et al. 1982).

In *Blastochloris* (previously called *Rhodopseudomonas*) *viridis, four* protein constituents were shown to compose the reaction center complex. The additional subunit was identified with a peculiar *c-type cytochrome containing tetraheme c groups*. The molecular masses of this cytochrome and subunits H, M, and L, obtained using SDS electrophoresis, were shown to be 38, 35, 28, and 24 kDa, respectively, this fact being the reason for the names given to non-cytochrome subunits H, M, and L. However, determination of the primary structure (which happened some years later) gave values of 40.5, 28.3, 35.9, and 30.6 kDa (336,

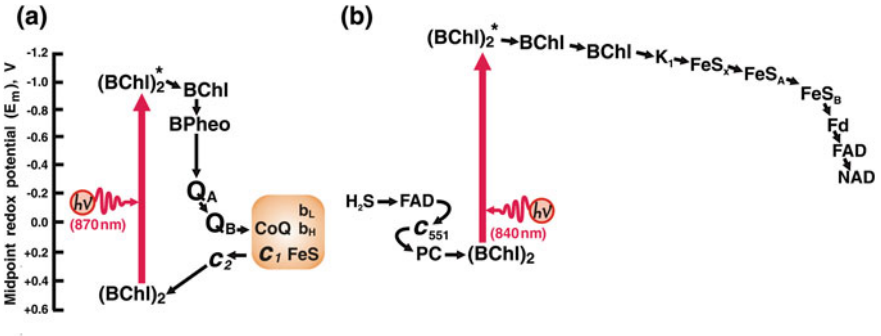

Fig. 2.6 Redox potentials of electron carrier involved in the photosynthetic systems of purple bacteria (**a**) and green sulfur bacteria (**b**). For explanations, see Sects. 2.1.1 and 2.2.2, respectively

258, 323, and 273 amino acid residues, respectively), which is in obvious contrast to the previously accepted nomenclature. The old subunits names are nevertheless still used in the literature.

The hydropathy profile of the M-subunit shows five very hydrophobic columns composed of at least 20 amino acid residues each. Each column is long enough to span the membrane in an α-helix. This conclusion was directly confirmed by X-ray analysis of *Blastochloris viridis* reaction center complexes (Hartmut Michel, Johann Deisenhofer, and Robert Huber, Nobel Prize in Chemistry, 1988, Fig. 2.7). They obtained 0.5–1-mm crystals of the complexes using $(NH_4)_2SO_4$ treatment of the reaction center complex solution supplemented with a detergent.

An X-ray study of these crystals revealed for the first time the *three-dimensional structure of a membrane energy transducer* at 0.3-nm resolution (Deisenhofer et al. 1984, 1985a, b). It was found that the 13-nm-long complex is composed of two peripheral domains (tetraheme cytochrome *c* and the H-subunit) and the central part (M- and L-subunits). It is the M- and L-subunits that bear bacteriochlorophylls and bacteriopheophytins of *b*-type, quinones, and nonheme iron that is connected to imidazoles of the four histidines of the protein. Comparing these data with earlier observations, one can assume that cytochrome *c* faces the periplasm, the H-subunit the cytoplasm, the M- and L-subunits being integrated in the hydrophobic membrane layer.

The X-ray picture of the reaction center complex reveals eleven transmembrane α-helical columns that are oriented perpendicular to the plane of the membrane and parallel to the long axis of the complex, being located in its middle (membrane) part. The H-subunit has only one α-helical column, while the M- and L-subunits, being similar to each other in their amino acid sequences and spatial structures, contain five such columns each. These columns are oriented symmetrically about the longitudinal axis of the complex (Fig. 2.8).

The single hydrophobic α-helix of the H-subunit serves as an anchor binding this hydrophilic polypeptide to the membrane. Another peripheral subunit, tetraheme cytochrome *c*, it is attached to the membrane by contacts with other subunits

Fig. 2.7 Nobel Laureates Hartmut Michel, Johann Deisenhofer, and Robert Huber

and by two fatty acids covalently bound to a glycerol residue forming a thioether bond with the SH group of the N-terminal cysteine of this cytochrome (Fig. 2.9).

When looking at the packing of polypeptide chains of the H-, M-, and L-subunits in the membrane, one should note complete absence of charged amino acids residues (Fig. 2.10a) and almost complete absence of bound water (Fig. 2.10b) in the transmembrane α-helical columns. Such amino acids and water are located on the membrane surfaces; the majority of the negatively charged residues are found on the outer membrane surface, whereas positively charged amino acids are exposed on the inner membrane surface. This fact suggests that the assembly of the reaction center complex polypeptides inside the membrane is directed by transmembrane $\Delta\Psi$ (the cell interior is negative). Electrophoresis of the protein domains is apparently involved in this assembly.

It should be noted that crystallization of the membrane proteins is extremely difficult to perform. The success in attempts to crystallize the *Bl. viridis* reaction center complex seems to be due to the fact that its central hydrophobic part (the M- and L-subunits) is to some extent protected from water by large hydrophilic polypeptides—the H-subunit and tetraheme cytochrome *c*.

Arrangement of Redox Groups. The most important result of the X-ray study of the *Bl. viridis* reaction center complex is that the arrangement of redox prosthetic groups is revealed (Deisenhofer et al. 1984). In Fig. 2.11, the results of the X-ray analysis of the complex is shown in such a way that only prosthetic groups are seen. According to these data, four cytochrome *c* hemes are located above the bacteriochlorophyll dimer. The Fe–Fe distances between the hemes are 1.4–1.6 nm. The Fe atom of the heme closest to $(BChl)_2$ is situated 2.1 nm above two Mg atoms of the bacteriochlorophyll dimer. The dimer is oriented parallel to the long axis of the reaction center complex. It is fixed between two α-helical *D* segments belonging to the M- and L-subunits (D_M and D_L, respectively). In each α-helical column there is a histidine residue, the imidazole group of which serves as an axial ligand for Mg^{2+} in $(BChl)_2$.

Two bacteriochlorophyll monomers were found to be arranged slightly below the dimer (the distance between Mg^{2+} ions in $(BChl)_2$ and BChl is 1.3 nm, and the

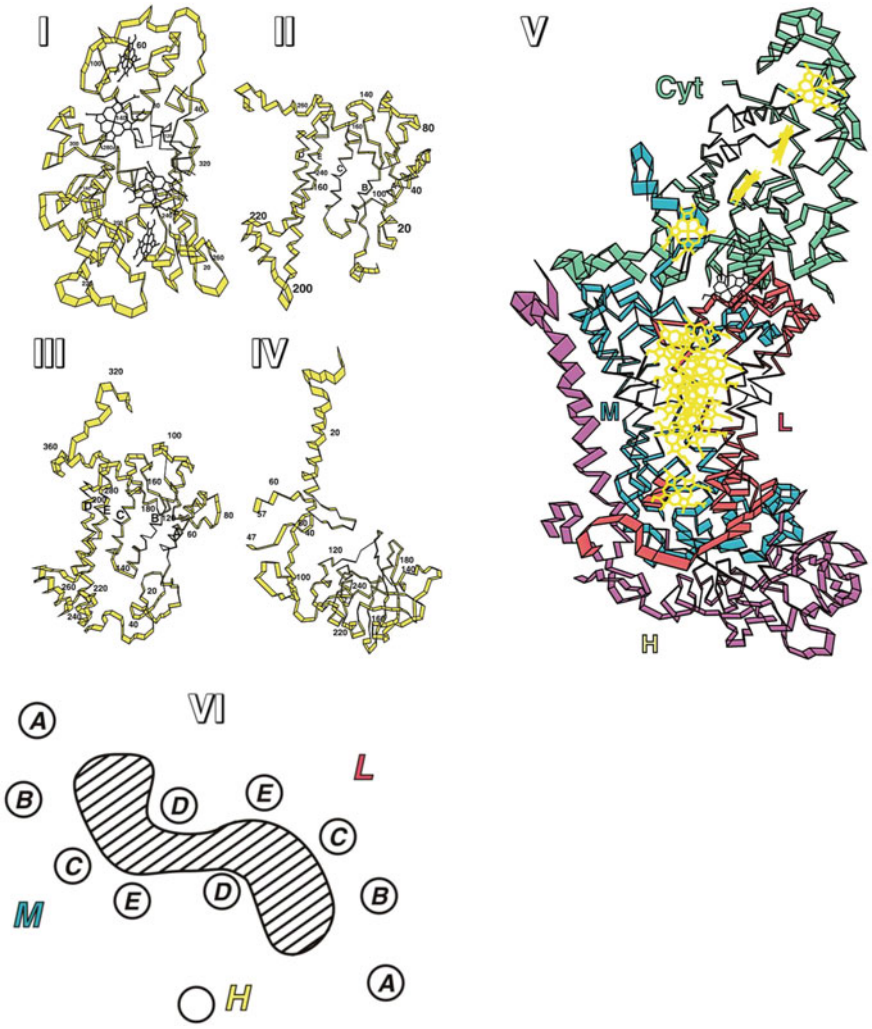

Fig. 2.8 Structure of protein subunits of the *Blastochloris viridis* reaction center: *I, II, III*, and *IV* stand for tetraheme cytochrome *c*, *L*-, *M*-, and *H*-subunits, respectively; *V*—general view of the reaction center complex; yellow electron-transporting prosthetic groups; *VI*—cross-section of the complex showing relationship between 11 α-helical segments (*top view*; A, B, C, D, E, five transmembrane α-helical segments of *M*- and *L*- subunits). The region occupied by the chromophores is shaded. The segments are tilted by an angle of 38° (segments *D*) and $< 25°$ (other segments) to the membrane plane. Figure section *VI* shows a section at a level close to the center of the hydrophobic membrane layer (Deisenhofer et al. 1984; Henderson 1985)

angles between the porphyrin ring planes are $\sim 70°$). Imidazoles of histidine residues located in C_M and D_M or C_L and D_L segment connections are ligands for Mg^{2+} of the monomers. Bacteriochlorophyll monomers are in contact with

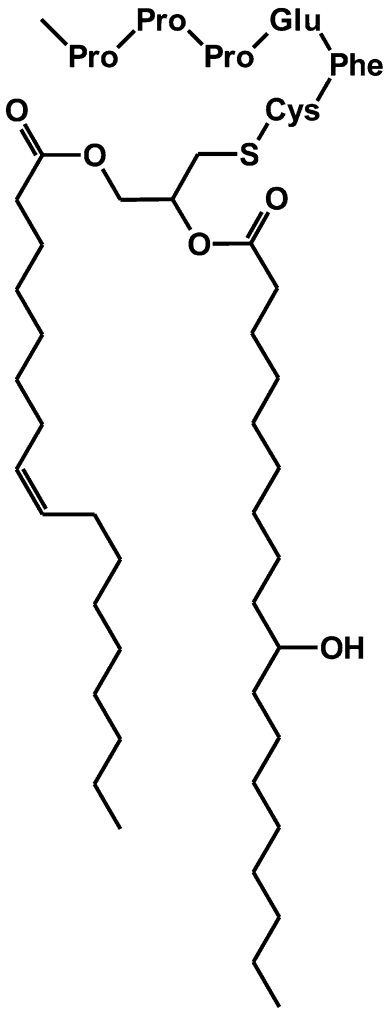

Fig. 2.9 Hydrophobic anchor of the tetraheme cytochrome *c* from *Blastochloris viridis*—fatty acid residues bound via glycerol to the SH-group of the N-terminal cysteine of the protein

bacteriopheophytins (BPheo). The corresponding distances and angles are 1.1 nm and 64°, respectively. Phytol residues participate in the formation of the contact. Menaquinone is located 1.8 nm below the BPheo molecule that is bound to the L-subunit. It lies on the *Trp-252* residue of the M-subunit. The symmetric position below another BPheo molecule is most probably occupied by the quinone "head" of CoQ, which is less tightly bound to the reaction center complex than menaquinone (it is released when the complexes are isolated and crystallized). This ubiquinone seems to lie on the *Phe*-216 residue of the L-subunit.

Halfway between the menaquinone and the ubiquinone pocket is a nonheme iron. It is connected with the protein in a manner other than that in other nonheme iron proteins. Four iron ligands were identified as imidazole groups of histidines of segments D_M, E_M, D_L, and E_L.

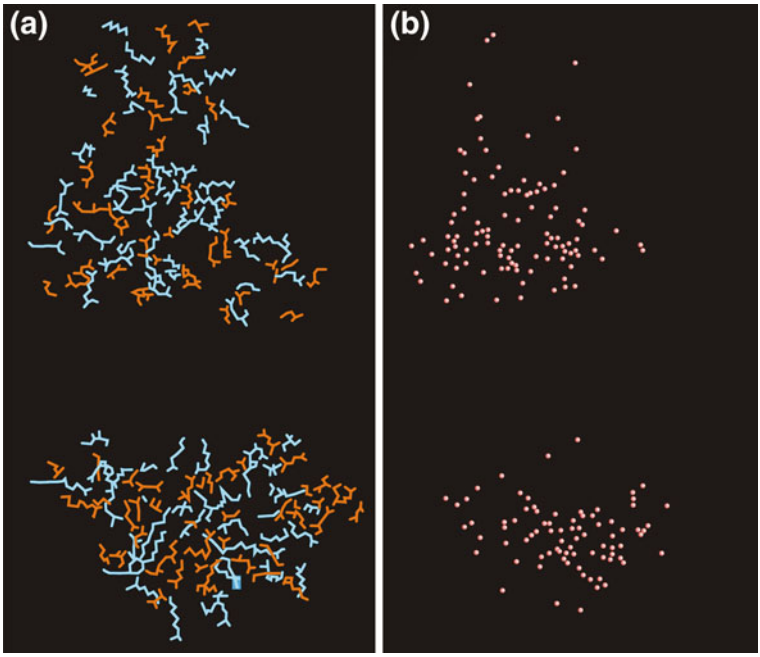

Fig. 2.10 Structure of reaction center complex of *Blastochloris viridis*. **a**—charged amino acid residues in the complex. Positively charged amino acids are orange, and negatively charged ones are blue. **b**—bound water molecules in the reaction center complex of *Bl. viridis*. The central part of the complex, which is immersed in the membrane, contains neither charged amino acid residues nor water, this fact being responsible for the sharp decrease in dielectric constant and, hence, small dissipation of energy occurring during the transmembrane electron transfer in this part of the complex (Deisenhofer et al. 1984)

Connections between segments A_M and B_M, C_M and D_M, A_L and B_L, and C_L and D_L as well as four of the five initial amino acid residues from the N-terminus of the H-subunit polypeptide are in contact with tetraheme cytochrome *c*. The *Tyr-L162* residue is located between $(BChl)_2$ and the nearest heme. It is supposed to participate in the electron transfer from this heme to the oxidized $(BChl)_2$. The *Glu-H177* residue, which has access to the CoQ pocket, is presumably involved in H^+ transfer from the cytoplasm to $CoQ^{\bullet -}$. Removal of the H-subunit was shown to exert a strong effect on the functioning of the reaction center at the level of CoQ.

According to spectral studies, the bacteriochlorophyll dimer is arranged perpendicularly to the plane of the *Bl. viridis* cytoplasmic membrane. Therefore, it seems highly probable that the long axis of the reaction center complex is arranged across the membrane. The distance between the Mg atoms of the bacteriochlorophyll dimer and the menaquinone is about 3.0 nm, so that an electron, running from the dimer to the quinone, crosses a major part of the hydrophobic barrier of the membrane.

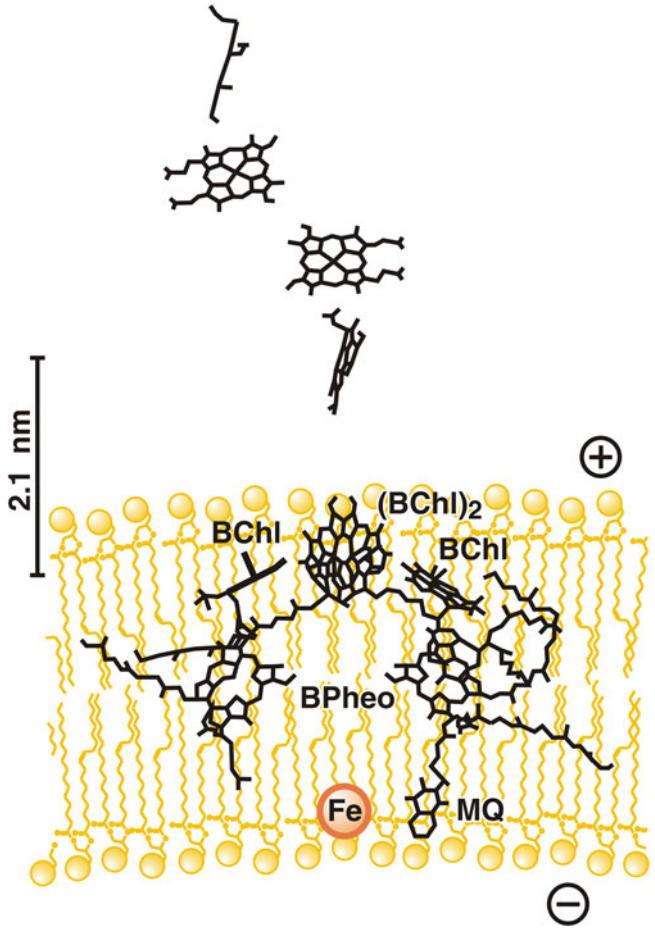

Fig. 2.11 Location of prosthetic groups in the reaction center complex of *Bl. viridis* (X-ray analysis data). Four hemes (above the membrane), bacteriochlorophyll dimer, two bacteriochlorophyll monomers, two bacteriopheophytins, menaquinone (MQ), and nonheme iron (Fe) are shown (Deisenhofer et al. 1984)

In general, the system composed of bacteriochlorophylls, bacteriopheophytins, and quinones resembles two parallel electron-transfer pathways. One can speculate that an electron reducing the bound ubiquinone (CoQ) to semiubiquinone ($CoQ^{\bullet -}$) goes along the right-hand pathway via the menaquinone, whereas the other electron reducing the semiquinone ($CoQ^{\bullet -}$) to ubiquinol passes via the left-hand pathway with no menaquinone involved. Experiments showed, however, that this is not the case—one of the pathways (the left one) does not participate in CoQ reduction (Parson 1982; Robert et al. 1985). When considering the possible function of this pathway, one should take into account the presence of a carotenoid molecule not far from the monomer BChl of the left branch. It is to this molecule

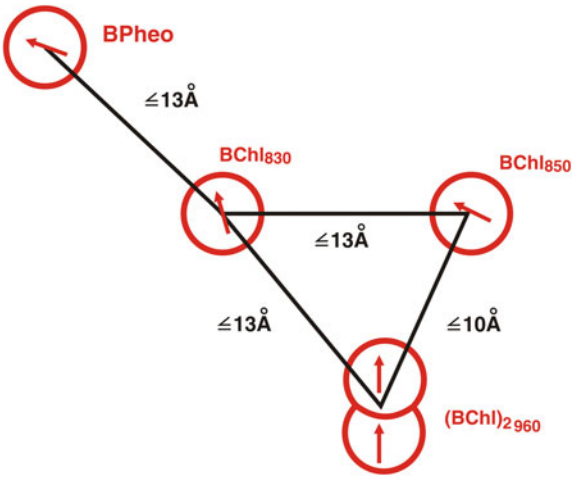

Fig. 2.12 Arrangement of chromophore components of *Bl. viridis* reaction center complex predicted on the basis of spectroscopic observations (Shuvalov and Asadov 1979)

that excitation of $(BChl)_2$ is transferred when $(BChl)_2$ is not oxidized by the right branch and is transformed instead from a singlet to the more stable triplet state. The excitation of the carotenoid is in turn dissipated through heat or emission of a light quantum of a longer wavelength (fluorescence). If oxygen manages to attack and oxidize the excited carotenoid, it leaves the reaction center complex so as to be exchanged for a new (intact) carotenoid molecule. In such way the carotenoid molecule "sacrifices itself" to save $(BChl)_2$, BChl, or BPheo, the oxidation of which would lead to irreversible inactivation of the whole complex.

To conclude this section, we note that the X-ray analysis data confirmed the chromophore arrangement scheme (Fig. 2.12) postulated by Shuvalov and Asadov in 1979 on the basis of optical spectroscopy (Shuvalov and Asadov 1979).

Sequence of Electron Transfer Reactions. The X-ray study shows the electron pathway through the reaction center complex to be determined by the spatial arrangement of redox groups:

$$(BChl)_2 \xrightarrow{h\nu} (BChl)_2^* \rightarrow BChl \rightarrow BPheo \rightarrow Q_A \rightarrow Q_B \qquad (2.1)$$

where in the case of *Bl. viridis* Q_A is MQ and Q_B is CoQ.

In fact, exactly the same sequence was suggested when picosecond-laser flash-induced changes in the light absorption of $(BChl)_2$, BChl, and BPheo were measured. The flash-induced excitation of $(BChl)_2$ was shown to be followed by oxidation of $(BChl)_2$ and reduction of BChl and BPheo. All these events are completed within 20 ps (Shuvalov and Duysens 1986; Shuvalov et al. 1986). Reduction of menaquinone by BPheo is the next step. It occurs with $t_{1/2}$ of about 230 ps. In the case of *Bl. viridis*, the $t_{1/2}$ for $(BChl)_2^{\bullet+}$ reduction to $(BChl)_2$ is about 270 ns (Fig. 2.13) (Matveetz et al. 1987).

It is crucial that the redox potential of a bacteriochlorophyll dimer in the nonexcited state (+440 mV) is substantially more positive when compared to the monomer potential (about –900 mV). The excitation of the dimer levels this

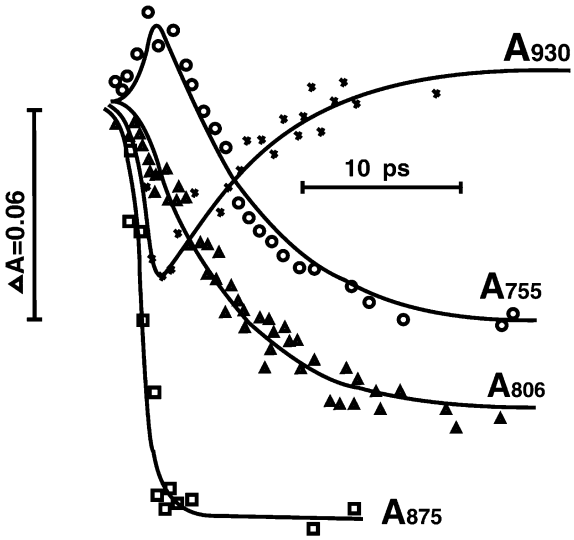

Fig. 2.13 Fast kinetics of light absorption changes (ΔA) in modified *Rhodobacter sphaeroides* reaction center complexes lacking one of two bacteriochlorophyll monomers ($BChl_M$). Absorption decrease at 930 nm (A_{930}) indicates formation of the excited bacteriochlorophyll dimer $(BChl)_2^*$; A_{875} decrease indicates formation of $(BChl)_2^+$. A_{805} decrease, reduction of bacteriochlorophyll monomer, $(BChl)_L$. A_{755} decrease, reduction of bacteriopheophytin, BPheo. Initial A_{775} increase is a result of the $(BChl)_2 \rightarrow (BChl)_2^*$ transition. Excitation was induced by a laser flash ($t_{1/2} = 0.2$ ps). (Matveetz et al. 1986)

difference. Its potential is about –950 mV, i.e. even slightly more negative than in the case of the nonexcited monomer, and even more so when compared to non-excited bacteriopheophytin (about –750 mV).

As shown in the group of one of this book's authors (V.P.S.), the heme of the tetraheme cytochrome *c*, serving as a $(BChl)_2^{\bullet+}$ reductant, is characterized by an α-band at 559 nm and a redox potential of about +380 mV (Dracheva et al. 1986). One can speculate that this heme is located just above $(BChl)_2$ in the reaction center complex. $Heme_{559}$ is, in turn, reduced by $heme_{556}$ (whose redox potential is about 310 mV). The electron donor for $heme_{556}$ is most probably water-soluble cytochrome c_2. The role of the two other hemes of the tetraheme cytochrome *c* (redox potentials +30 mV and –50 mV) remains obscure.

The most remarkable feature of the primary processes of photosynthetic electron transfer is their extremely fast rates. These processes represent *the fastest chemical reactions known in biological systems thus far*. As a result, the first intermediates of the photoredox chain are very short-lived, which is needed to prevent their oxidation by oxygen.

In *Bl. viridis*, anion-radical $MQ^{\bullet-}$ is the first intermediate that has a turnover rate comparable to that of the intermediates of the majority of enzymatic processes. Oxidation of $MQ^{\bullet-}$ by bound CoQ takes about 0.1 ms. Therefore, MQ is often

described as a *primary electron acceptor*. In some bacteria, this role is played not by MQ, but also by CoQ. In these cases the reaction center complex contains two molecules of CoQ—the primary acceptor CoQ_A and the secondary acceptor CoQ_B.

Electron transfer between the two quinones is facilitated by the presence of a nonheme iron that does not undergo oxidoreduction and persists in the Fe^{2+} form. In fact, Mn^{2+} can effectively substitute for Fe^{2+} in the reaction center complex (Okamura et al. 1982).

From one point of view, when looking at the mechanism of electron transfer in the reaction center complex, $CoQ_B^{\bullet-}$ can be considered the final product of the operation of the complex:

$$Q_A^{\bullet-} + Q_B \rightarrow Q_A + Q_B^{\bullet-} \tag{2.2}$$

More probable, however, is that not only Q_B, but also $Q_B^{\bullet-}$ is reduced by $Q_A^{\bullet-}$ (see Eq. 2.3). Supporting this version, one should note that the affinity of $Q_B^{\bullet-}$ for the L-subunit of the photosynthetic reaction center complex is much higher than that of Q_B and Q_BH_2.

Reduction of Q_B is accompanied by addition of two protons:

$$Q_A^{\bullet-} + Q_B^{\bullet-} + 2\ H^+ \rightarrow Q_A + Q_BH_2 \tag{2.3}$$

Mechanism of $\Delta\bar{\mu}_{H^+}$ Generation. Because *cytochrome c_2 and quinone are located on the opposite sides of the membrane* (Okamura et al. 1982; Deisenhofer et al. 1984), the transfer of reducing equivalents is directed through the membrane to its cytoplasmic surface. Assuming that it is an electron that moves from cytochrome c_2 to quinone, one can predict that the cytoplasm should be charged negatively relative to the periplasm or the interior of the chromatophore.

This prediction was confirmed by a series of observations concerning $\Delta\Psi$ generation by the reaction center complexes. To monitor $\Delta\Psi$, L. Drachev, A. Kaulen, and A. Semenov in our group developed a method that made it possible to *carry out direct voltmeter measurements of $\Delta\Psi$ generated by enzymes built into proteoliposomes* (Drachev et al. 1974, 1979). The term "proteoliposome" was suggested by one of the authors of this book (V.P.S.) in 1972 for closed membrane vesicles that could be obtained as a result of self-assembly from phospholipids and proteins (Skulachev 1972; Kayushin and Skulachev 1974). In these experiments, proteoliposomes were sorbed on one of the surfaces of a collodion film that was soaked with a solution of phospholipids in decane.

The experiments showed that proteoliposomes are sorbed in such a way that their inner solution does not mix with the outer one (Severina 1982). It is likely that during sorption a part of the proteoliposome membrane that is in contact with the film is dissolved by the decane the film is soaked with, while other parts of the membrane remain intact, thus forming a barrier between the inner solution of the film-attached proteoliposome and the outer solution surrounding the film.

The generation of $\Delta\Psi$ on the membrane of sorbed proteoliposomes can be registered by a voltmeter by using two electrodes that are placed on the two sides of the collodion film. The time resolution of this system is about 50 ns, which is

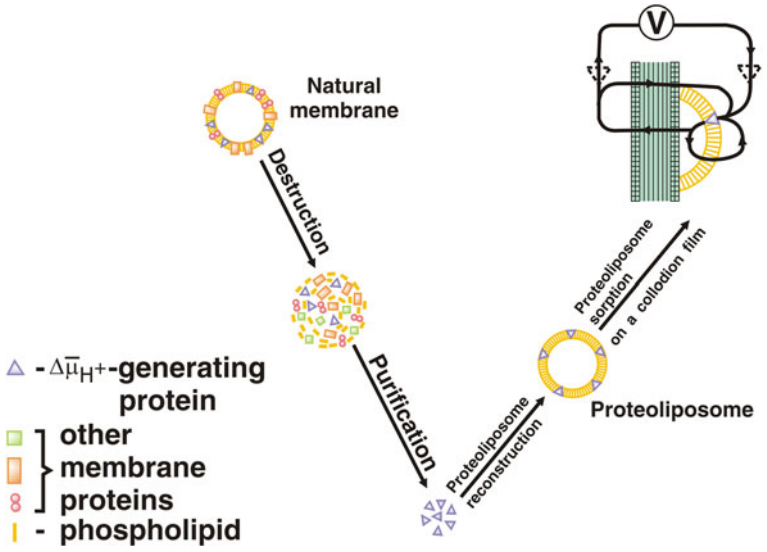

Fig. 2.14 General scheme of studies on $\Delta\bar{\mu}_{H^+}$-generating proteins: purification, self-assembly, and direct measurement of their electrogenic activity (Skulachev 1988)

much shorter than a single turnover rate of any $\Delta\bar{\mu}_{H^+}$. So this method can be used not only to register very fast $\Delta\Psi$ generation, but also to resolve its separate stages. In other words, it is possible to register transfer of a charge (e.g. an electron or a proton) inside the molecule of a protein generating $\Delta\bar{\mu}_{H^+}$.

Figure 2.14 presents a general scheme of the study of $\Delta\bar{\mu}_{H^+}$—generating proteins. It includes their purification, self-assembly, and finally direct measurement of the function of these proteins—transformation of light or chemical energy into electrical form.

Our method made it possible to measure $\Delta\Psi$ generation by reaction centers on nanosecond and microsecond time scales. The main contribution to $\Delta\Psi$ generation was found to be a process that is faster than 50 ns (the time resolution of the measuring system). In the reaction sequence, such fast kinetics is inherent in steps between $(BChl)_2$ and Q_A. Combining this observation with the transmembrane arrangement of the , one can infer that the transfer of reducing equivalents between the $(BChl)_2$ and the quinone is electrogenic, i.e. the electron transfer is not compensated by the movement of other charged component(s) (Dracheva et al. 1986).

The superfast monitoring of $\Delta\Psi$ generation by the *Bl. viridis* cells by electric measurements of the light-gradient type was done by H. Trissl and coworkers (Deprez et al. 1986). The $\Delta\Psi$ measured by this indirect method is lower in magnitude than in our experiments by a factor of at least 100, but the time resolution appears to be as good as 40 ps. Two electrogenic phases ($t_{1/2} \leq 40$ ps, $t_{1/2} = 125$ ps) of almost equal contributions were observed. The first phase corresponded to BPheo reduction by $(BChl)_2$ and the second to BPheo oxidation by menaquinone.

In addition to the fast electrogenic phases, we discovered three slower phases (Dracheva et al. 1986). One appeared when the decane solution of phospholipids used to impregnate the film was supplemented with CoQ_{10}. The magnitude of the phase was about 5 % of the overall $\Delta\Psi$ generated after a laser flash. The time constant of this process was 400 μs, i.e. somewhat slower than the Q_B reduction rate. It was sensitive to *o*-phenanthroline, an inhibitor of Q_B reduction. We concluded that the slow electrogenic phase is somehow associated with reduction of Q_B. Decane apparently extracts Q_B from the chromatophores or proteoliposomes attached to the collodion film saturated with this hydrocarbon, the effect being prevented by added CoQ_{10}.

There are two possible mechanisms of this slow electrogenic phase that requires CoQ_{10}. (1) Electron transfer from Q_A to Q_B is electrogenic. (2) There is a proton-conducting path from the membrane surface to Q_B—protons move along this path to the reduced anion Q_B and combine with this anion, thus forming QH_2.

To discriminate between these two possibilities, we studied the effect of two consecutive 15-ns laser flashes. If the first version were correct, both flashes would be effective in slow electrogenesis. If the second mechanism were operative, only the second flash would be effective since the $CoQ^{\bullet -}$ formed after the first flash cannot bind H^+ at physiological pH. It is only after the addition of the second electron (which can happen after the second laser flash) that protonation can occur.

As shown in Fig. 2.15, the second flash, but not the first, induced the slow electrogenic phase. This means that version (2) is valid, i.e. the slow electrogenic phase is due to H^+ transfer from water to the place inside the reaction center complex where Q_B is located. If we presume that the dielectric properties of the membrane hydrophobic barrier are the same throughout its entire depth, it becomes possible to define what fraction of this barrier is crossed by H^+. Since the slow stage constitutes 5 % of the entire electric response caused by transmembrane charges transfer, one might assume that the proton is transferred by 1/20 part of the membrane depth. Further research, however, proved the real situation to be more complicated (we will discuss it later).

To study the contribution of the tetraheme cytochrome *c*, conditions were used when two hemes (c_{556} and c_{559}) were reduced. No CoQ was added to avoid electrogenic effects accompanying formation of $CoQH_2$. A laser flash that photooxidized $(BChl)_2$ was found to induce temporary oxidation of these hemes ($t_{1/2}$ of about 300 ns for heme c_{559} and about 3 μs for heme c_{556}). This process was accompanied by an additional biphasic electrogenesis. The kinetics of each of the phases corresponded to the kinetics of heme oxidation. The contributions of these fast and slow cytochrome electrogenic phases to the overall $\Delta\Psi$ generation by the reaction center complex were about 15 and 5 %, respectively (Fig. 2.16).

A scheme illustrating the structure–function relationships in the *Bl. viridis* reaction centers is shown in Fig. 2.17. The distances between redox groups are given according to the X-ray data. It is interesting that H^+ transfer from the cytoplasmic membrane surface to CoQ constitutes only 5 % of the overall $\Delta\Psi$. There are two possible explanations for this fact—either the proton path (from water to CoQ) is shorter than the path of an electron (from cytochrome *c* to CoQ),

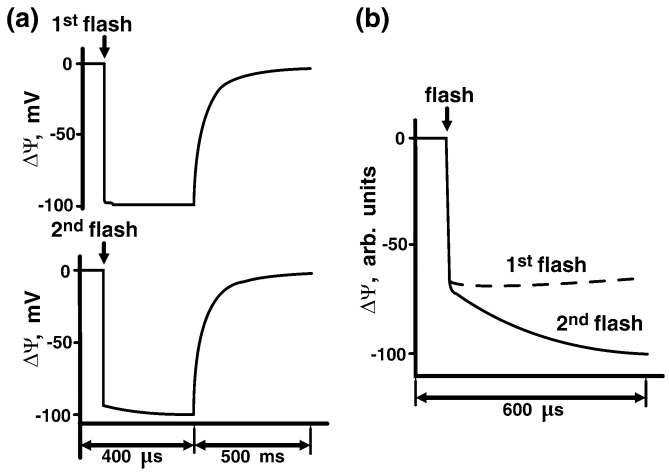

Fig. 2.15 Generation of ΔΨ by *Bl. viridis* reaction center complexes in response to two consecutive 15-ns laser flashes. The time between flashes was 0.5 s. Only the second flash generates a "slow" electrogenic phase developing on the microsecond time scale (**a**). This phase is shown at higher resolution in (**b**), where dashed and solid lines represent the first and second flashes, respectively. ΔΨ was measured with the proteoliposome-collodion film system. CoQ_{10} was added to the solution used to impregnate the film. The redox potential of the medium was +240 mV. (Dracheva et al. 1986)

or H^+ ions are transferred through a less hydrophobic part of the complex. Most likely both factors contribute to this phenomenon. It seems quite probable that a similar situation occurs during the stages of electron transfer.

The distances between Q_A and $(BChl)_2$, $(BChl)_2$ and c_{559}, and c_{559} and c_{556} along the axis vertical to the membrane plane are 2.9, 2.1, and 1.2 nm, respectively. If the electrogenesis were a linear function of the distance between the redox groups involved, the relative contributions of these electron transfer steps would be 1:0.7:0.4. In fact, they were found to be 1:0.2:0.7. This means that the contribution is greater when the electron transfer stage is immersed deeper into the membrane. This pattern becomes quite understandable when we take into account the fact that the membrane dielectric constant value increases approaching the water phase (Skulachev 1988).

In the 1960s, when Peter Mitchell formulated his chemiosmotic hypothesis, he suggested that an electron moving from cytochrome *c* to CoQ via bacteriochlorophyll crosses the hydrophobic membrane barrier (*the electron transfer half-loop*) (Mitchell 1966). This assumption, quite speculative at that time, has now been directly proved. The only new point that was detected in the result of experimental trial of the original Mitchell scheme is that besides the electron transfer across the membrane, there is a small but measurable electrogenic phase arising because of the movement of the proton in the opposite direction (this movement being necessary for formation of $CoQH_2$ from CoQ) (Skulachev 1988).

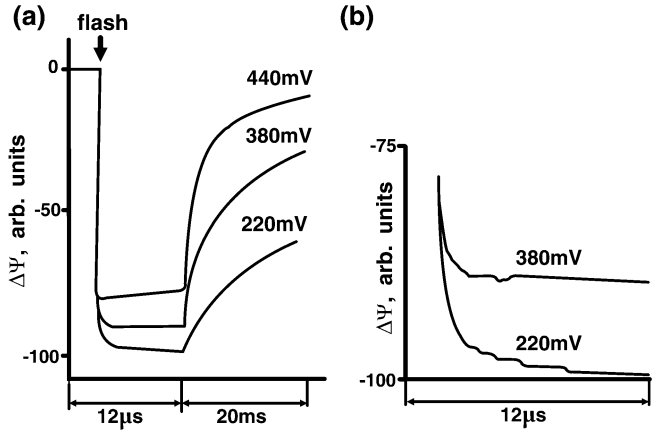

Fig. 2.16 Generation of ΔΨ by *Bl. viridis* reaction center complexes—the role of high-potential hemes of cytochrome *c*. Measurements were carried out at redox potential of the medium equal to +220 mV (two high-potential hemes of the tetraheme cytochrome *c* were reduced and two low-potential hemes were oxidized), +380 mV (one of high-potential hemes was 50 % reduced), and +440 mV (all four hemes were oxidized). The figure to the right (b) shows part of figure (a) in more detail. (Dracheva et al. 1986)

2.1.3 $CoQH_2$: Cytochrome c-Oxidoreductase

$CoQH_2$: cytochrome *c*-oxidoreductase (other names, Complex III and bc_1 complex) was discovered and studied in detail when the mitochondrial respiratory chain was investigated (see Sect. 4.3). Later, it was described in photoredox chains. There are still scanty information on the molecular properties of the constituents of the bc_1 complex in photosynthetic bacteria. However, almost all that is known about it is in agreement with that previously reported for its mitochondrial analog. That is why in this section only a short description of the bacterial bc_1 complex will be given.

The bc_1 complex comprises cytochrome *b* containing two hemes—the low-potential heme b_L (another name b_{556}, since its α-peak in the absorption spectrum is located at 556 nm) and the high potential heme b_H (or b_{560}), one iron–sulfur center (FeS_{III}), one cytochrome c_1, and several colorless protein subunits without any prosthetic groups. $CoQH_2$ and cytochrome c_2 serve as the reductant and the oxidant of the bc_1 complex, respectively. Cytochrome c_2 is a water-soluble cytochrome similar to mitochondrial cytochrome *c*. In reconstituted systems, mitochondrial cytochrome *c* can substitute for cytochrome c_2 (see Fig. 2.6 for the potentials of these redox carriers).

The $CoQH_2$:cytochrome *c*-oxidoreductase complex is *the slowest component of the photosynthetic redox chain*. Its maximal turnover in situ is generally around once per 10 ms (Rich 1984).

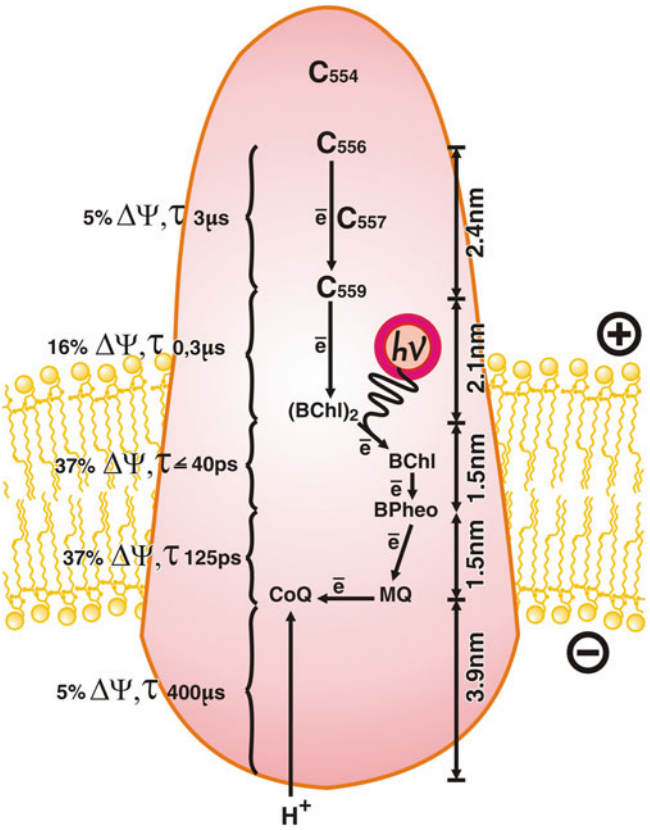

Fig. 2.17 Mechanism of electrogenic phases in *Bl. viridis* reaction center complex (Dracheva et al. 1986; Skulachev 1988)

By analogy with the more elaborate mitochondrial complex, one can suppose that $\Delta\bar{\mu}_{H^+}$ generation by this system is partially due to the electron transfer from heme b_L to b_H, directed perpendicularly to the membrane plane, as shown in Fig. 2.4. This process is oriented in the direction of the cytoplasmic surface of a bacterial membrane. An electron was shown to cross 35–40 % of the membrane thickness while moving from heme b_L to b_H (Glaser and Crofts 1984). The rest is assumed to be crossed by H^+ ions moving in the direction opposite to that of an electron (see Fig. 2.4).

It remains unclear whether CoQ, $CoQ^{\bullet-}$, or both serve as electron acceptor(s) for cytochrome b_H. If this function is specific only for one of these components, it means that formation of a completely reduced form of ubihydroquinone ($CoQH_2$) must involve the dismutation reaction ($2\ CoQ^{\bullet-} + 2\ H^+ \leftrightarrow CoQ + CoQH_2$). The reaction center complex is another source of electrons for CoQ reduction to $CoQH_2$. Steady-state functioning of the system requires that for each two CoQ

molecules reduced to $CoQH_2$, one would be reduced by the reaction center and the other by b_H heme. Protons required to convert CoQ to $CoQH_2$ are in both cases transported from the cytoplasm.

Having been formed, $CoQH_2$ crosses the greater part of the hydrophobic membrane barrier to be oxidized by FeS_{III}. As a result, $CoQ^{\bullet -}$, reduced FeS_{III}, and 2 H^+ are formed, the latter being transported through the remainder of the hydrophobic barrier to be released to the periplasm or chromatophore interior. In the case of *Rh. rubrum* and *Rhodobacter sphaeroides*, electron transfer from FeS_{III} to $(BChl)_2$ via cytochrome c_1 and cytochrome c_2 completes the cycle, as shown in Fig. 2.4. In *Bl. viridis*, tetraheme cytochrome *c* participates in the electron transfer between cytochrome c_2 and $(BChl)_2^{\bullet +}$.

The reaction sequence catalyzed by the $CoQH_2$:cytochrome *c*-oxidoreductase, as shown in Fig. 2.4, represents, in fact, a version of the Q-cycle scheme postulated by Mitchell (Mitchell 1975). The key postulate of this scheme was that $CoQH_2$ oxidation and CoQ reduction occur in such a manner that the fate of each of the two electrons removed from $CoQH_2$ or added to CoQ appears to be different. Now this suggestion is firmly established at least for $CoQH_2$ oxidation. *FeS_{III} was shown to act as a $CoQH_2$ oxidase, whereas heme b_L of cytochrome b was shown to serve as an oxidase of $CoQ^{\bullet -}$, the latter being formed from $CoQH_2$*. There is a chemical reason for the fact that $CoQH_2$ and $CoQ^{\bullet -}$ are oxidized by different enzymes—the redox potentials of hydroquinone and semiquinone are quite different (Rich 1984).

It is noteworthy that the binding of $CoQH_2$ to the FeS_{III} protein proceeds in such a way that the hydroquinone "head" of $CoQH_2$ is bound near a positively charged group (presumably Fe^{3+}). This induces an acidic shift of the pK value of $CoQH_2$, which makes its deprotonation easier. Having lost a proton, $CoQH_2$ changes into $CoQH^-$, which is oxidized by FeS_{III}. Deprotonation seems to be necessary for this oxidation reaction since the redox potential of *the $CoQH_2$/$CoQH_2^{\bullet +}$* couple is higher than +850 mV, while that of $CoQH^-/CoQH^{\bullet}$ couple is +190 mV (Rich 1984), which is more negative than that of FeS_{III}.

In mitochondria, electron transfer from ubiquinol to *FeS_{III}* and then via cytochrome c_1 to cytochrome *c* is catalyzed by respiratory chain complex III, which is also known as bc_1 complex or ubiquinol:cytochrome *c*-oxidoreductase. This complex has been found in a number of bacteria; in many respects it is similar to plastoquinol:plastocyanin-oxidoreductase of thylakoids (*bf* complex). Redox groups of the bc_1 complex include an [2Fe − 2S] cluster, which is part of a so-called Rieske protein, two hemes of a *b*-type cytochrome and a cytochrome c_1 heme. The [2Fe–2S] cluster of the Rieske protein is connected to the polypeptide by the bonds of one iron atom to two cysteine residues and of the other iron atom to two histidine residues. Thus, the FeS cluster is part of the inner globular structure of the polypeptide chain that is anchored in the membrane with its hydrophobic N-terminal helix and is protruded from the lipid bilayer into the water phase.

Cytochrome c_1 has a globular domain similar to the Rieske protein and a hydrophobic anchor that is located on the C-terminus of the protein. The cytochrome b subunit has eight transmembrane α-helices. Four conserved histidine residues are arranged in pairs on each of two helices so as to serve as axial ligands to the heme (Crofts and Wraight 1983; Rich 1984).

2.1.4 Ways to Use $\Delta\bar{\mu}_{H^+}$ Generated by the Cyclic Photoredox Chain

The proton potential generated in chromatophores by the cyclic redox chain can be used to perform *four types of chemical work*: (1) *ATP formation* from ADP and inorganic phosphate by H^+- ATP synthase; (2) *formation of inorganic pyrophosphate* from two molecules of inorganic phosphate by H^+-pyrophosphate synthase; (3) *reverse transfer of reducing equivalents* via the NADH:CoQ-oxidoreductase complex from the hydrogen donors of about a zero redox potential to NAD^+; and (4) reduction of $NADP^+$ by NADH catalyzed by *transhydrogenase*.

NADH:CoQ-oxidoreductase is the first (of three) $\Delta\bar{\mu}_{H^+}$ generators in the respiratory chain. When operating in the opposite direction ($CoQH_2 \rightarrow NAD^+$), this enzyme consumes $\Delta\bar{\mu}_{H^+}$ produced by the photosynthetic redox chain in chromatophores. This makes it possible to reduce NAD^+ (redox potential − 320 mV) by such hydrogen donors as H_2S (redox potential about 0 mV). The formed NADH is used later in reductive biosyntheses.

One of the ways to utilize NADH is to reduce $NADP^+$ in a transhydrogenase reaction. The $\Delta\bar{\mu}_{H^+}$-consuming enzyme transhydrogenase is also located in the chromatophore membrane. When consuming $\Delta\bar{\mu}_{H^+}$, transhydrogenase strongly increases the redox potential of the $NADPH/NADP^+$ couple, an effect favorable for those reductive syntheses that use NADPH as a hydrogen donor.

In the dark, NADH:CoQ-oxidoreductase can operate in the forward direction oxidizing NADH by CoQ, a process coupled to $\Delta\bar{\mu}_{H^+}$ generation. The formed $CoQH_2$ is further oxidized by the bc_1 complex which reduces cytochrome c_2 and produces $\Delta\bar{\mu}_{H^+}$. Cytochrome c_2 in turn reduces cytochrome o, which transfers electrons to O_2 and generates $\Delta\bar{\mu}_{H^+}$. Thus, purple photosynthetic bacteria have a respiratory chain with three $\Delta\bar{\mu}_{H^+}$ generators, and it starts to operate when light is unavailable.

The cytoplasmic membrane of photosynthetic bacteria has some additional $\Delta\bar{\mu}_{H^+}$consumers that are absent from chromatophores, i.e.: (1) H^+ motors that rotate bacterial flagella; (2) H^+ that allow accumulation of metabolites in the bacterial cell; (3) Na^+, K^+-transport systems responsible for the asymmetrical distribution of these ions across the cytoplasmic membrane. Gradients of Na^+ and K^+ ions function as a $\Delta\bar{\mu}_{H^+}$-buffer. A similar function seems to be served by pyrophosphate.

A general scheme of light energy transduction to various types of work in the cytoplasmic membrane of purple bacteria is shown in Fig. 2.18.

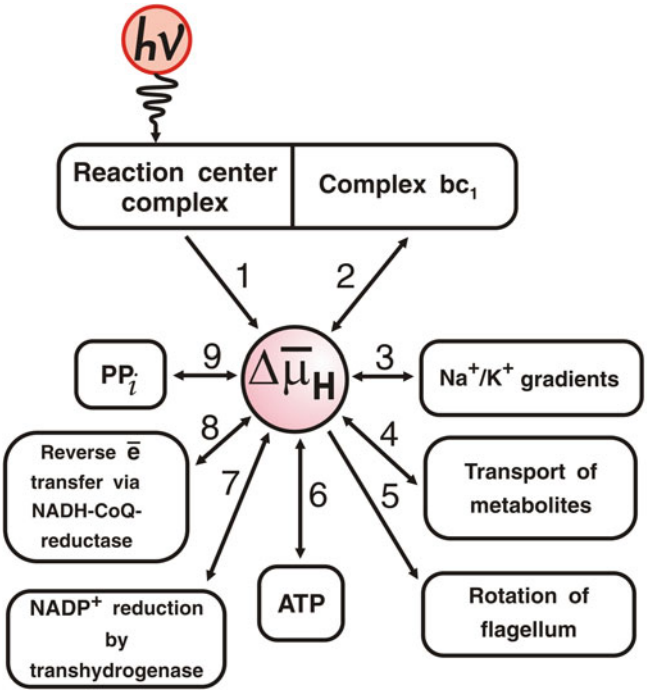

Fig. 2.18 Light-dependent energy transductions in the cytoplasmic membrane of purple photosynthetic bacteria (1–9). In the chromatophore membrane of the same bacteria, a simplified energy transduction pattern occurs when pathways 4, 5, and possibly 3 are absent (Skulachev 1988)

2.2 Noncyclic Photoredox Chain of Green Bacteria

In the preceding section it was mentioned that purple photosynthetic bacteria can reduce NAD^+ by H_2S at the expense of light energy converted to $\Delta\bar{\mu}_{H^+}$by the cyclic redox chain. Another mechanism is employed by green anaerobic photosynthetic bacteria. It is organized such that *the light simultaneously causes* $\Delta\bar{\mu}_{H^+}$ *generation and* NAD^+ *reduction by hydrogen sulfide*.

This mechanism is the simplest version of the so-called *noncyclic photosynthetic redox chain*. Its tentative scheme is shown in Fig. 2.19. In this case the reaction center complex is similar to the photosystem 1 complex of chloroplasts and cyanobacteria (this chapter, Sect. 2.3.2), but the core of the reaction center consists of a homodimer of one subunit instead of a heterodimer of two homologous subunits in the case of photosystem 1. Bacteriochlorophyll dimer, two bacteriochlorophyll monomers, vitamin K_1 (phylloquinone or menaquinone), and three FeS clusters (FeS_X, FeS_A, and FeS_B) that are included sequentially in the redox chain that constitutes the reaction center complex. The water-soluble FeS protein ferredoxin (Fd), which is located on the cytoplasmic surface of the

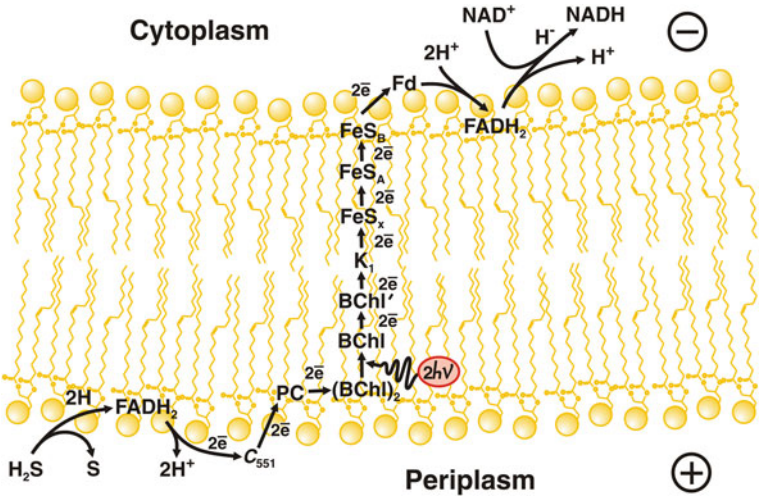

Fig. 2.19 Noncyclic photosynthetic redox chain of green sulfur bacteria (Hauska et al. 2001). Explanations are provided in the text

membrane, serves as an electron acceptor. Electrons are transferred from Fd to a flavoprotein (with FAD prosthetic group) and then to NAD^+.

Photooxidized $(BChl)_2^{\bullet+}$ is reduced by the donor segment of the redox chain starting from H_2S. The segment contains flavoprotein with FAD as a prosthetic group, cytochrome c_{551}, and Cu-containing protein plastocyanin (PC). The redox potentials of the main components of this redox chain have already been shown in Fig. 2.6b.

The photoelectrogenic activity of the redox chain of green bacteria was registered in experiments with membrane fragments associated with a planar phospholipid membrane. The mechanism of this effect consists, as in other chlorophyll-containing $\Delta\bar{\mu}_{H^+}$ generators, of a transmembrane electron transfer. The electron transfer shown in Fig. 2.19 must be accompanied by H^+ release to the outer medium due to the oxidation of H_2S to sulfur by the electron donor segment of the redox chain, which is located close to the outer surface of the membrane. On the opposite (inner, i.e. cytoplasmic) side of the membrane, H^+ uptake should occur, since NAD^+ is reduced by the bacteriochlorophyll system that can donate electrons—not protons. To form NADH from NAD^+, one H^+ per two electrons accepted by NAD^+ must be consumed.

Thus, on the *outer membrane surface* of green bacteria the following reaction takes place:

$$H_2S \rightarrow S + 2\,H^+ + 2\bar{e}, \tag{2.4}$$

while the process occurring on the *inner membrane surface* can be described as:

$$NAD^+ + H^+ + 2\bar{e} \rightarrow NADH. \tag{2.5}$$

It should be noted that *both* $\Delta\bar{\mu}_{H^+}$ *generation and NAD*$^+$ *reduction are carried out by one and the same light-driven redox chain* (for review, see (Hauska et al. 2001)).

It should be mentioned that the described metabolic pattern (see Fig. 2.19) is characteristic of only *anaerobic* green sulfur bacteria, such as *Chlorobium sps*. In contrast, *facultatively aerobic* green bacteria (e.g. of the *Chloroflexus* genus) have a redox chain more similar to that found in the purple bacteria (for review see (Merchant and Sawaya 2005)).

2.3 Noncyclic Photoredox Chain of Chloroplasts and Cyanobacteria

The noncyclic photosynthetic redox chain of cyanobacteria and chloroplasts resembles that of the green bacteria. It also utilizes light to form $\Delta\bar{\mu}_{H^+}$ and to reduce NAD(P)$^+$ by an electron donor of a more positive redox potential. The main specific feature of cyanobacteria and chloroplasts compared to green bacteria is that water (instead of hydrogen sulfide) is utilized as the electron donor. The redox potential difference between NADP$^+$ and H_2O is about 1.2 V, i.e. much larger than that between NAD$^+$ and H_2S used by the green bacteria (0.3 V). Therefore, the transport of one electron along the chloroplast (cyanobacterial) redox chain requires two photons to be consumed, instead of one photon as in the green bacteria.

In plant cells the photosynthetic redox chain is located in the intrachloroplast membranes, mainly in *thylakoids*, i.e. closed, flattened membrane vesicles stacked in batches called *grana* that can be connected by extended membrane structures (lamellas of the chloroplast stroma) (Fig. 2.20). Thylakoids are also found in many cyanobacteria.

2.3.1 Principle of Functioning

A simplified version of the light-dependent redox chain in the thylakoid membrane of chloroplasts is given in Fig. 2.21. The chain includes two types of reaction centers (they are called photosystems 1 and photosystems 2) and several enzymes catalyzing the dark reactions of water oxidation, Q-cycle, and NADP$^+$ reduction.

The process is initiated by absorption of a photon by antenna chlorophyll. Excitation migrates from the antenna chlorophyll to the chlorophyll of a photosystem. If this is the *chlorophyll dimer of photosystem 2* (absorption maximum at 680 nm), it is oxidized by a monomer of chlorophyll II; an electron then moves to *pheophytin*. From pheophytin the electron is transferred to the bound plastoquinone (PQ_A). Then the electron reaches another bound plastoquinone molecule (PQ_B). Similarly to bacterial photosynthesis, this process is catalyzed by nonheme

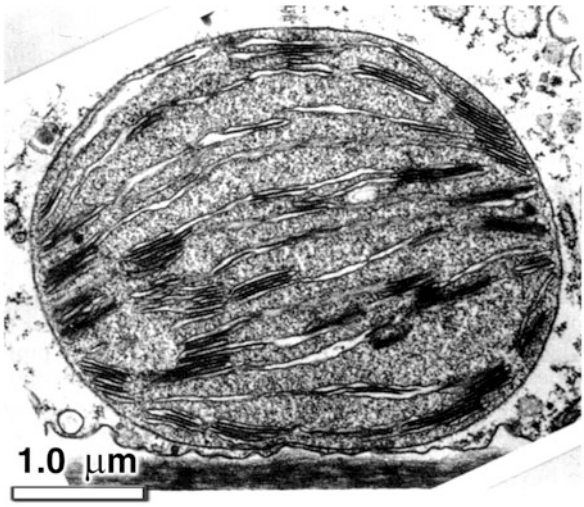

Fig. 2.20 Structure of chloroplast

iron connected to four imidazoles of histidines residues of the protein. The chlorophyll cation radical $(ChlII)_2^{\bullet+}$ accepts an electron from one of the tyrosine residues of the protein, which, in turn, is reduced by an electron removed from a H_2O molecule by means of a rather complicated *manganese-containing water-oxidizing complex* (WOC). Electrons, molecular oxygen, and protons are released when the water molecule is oxidized. The released protons appear in the intrathylakoid space. The reduced PQ is oxidized by the PQH_2:plastocyanin-oxidoreductase (also called b_6f complex, which is a chloroplast analog of the bacterial and mitochondrial bc_1 complex). The b_6f complex comprises a three-heme cytochrome *b* (hemes b_L, b_H, and c_i), FeS_{III}, and cytochrome *f*, which is functionally similar to cytochrome c_1.

The b_6f complex catalyzes a Q-cycle similar to that described in purple bacteria and mitochondria. As a result, the transport of one electron from PQ to cytochrome *f* is coupled to the translocation of one charge across the thylakoid membrane, the absorption of two H^+ ions from the chloroplast stroma, and the release of two H^+ ions into the thylakoid interior. These protons are taken up on the outer surface of the thylakoid membrane and are released on its inner surface.

From cytochrome *f* the electron moves to the copper-containing protein plastocyanin (Pc), which reduces the cation radical of the chlorophyll dimer of photosystem 1 (in the ground state, the absorption maximum for this chlorophyll is near 700 nm). The $(ChlI)_2^{\bullet+}$ radical cation is formed as a result of the oxidation of the excited $(ChlI)_2^*$. The electron taken from $(ChlI)_2^*$ is transferred via the chlorophyll monomers (ChlI and ChlI′) and vitamin K_1 (phylloquinone) to the *iron–sulfur center* FeS_X, which acts as the primary stable electron acceptor in photosystem 1.

During the next stages the electron is transported to other iron–sulfur clusters (FeS_B, FeS_A, and ferredoxin) and further to a flavoprotein containing FAD as the

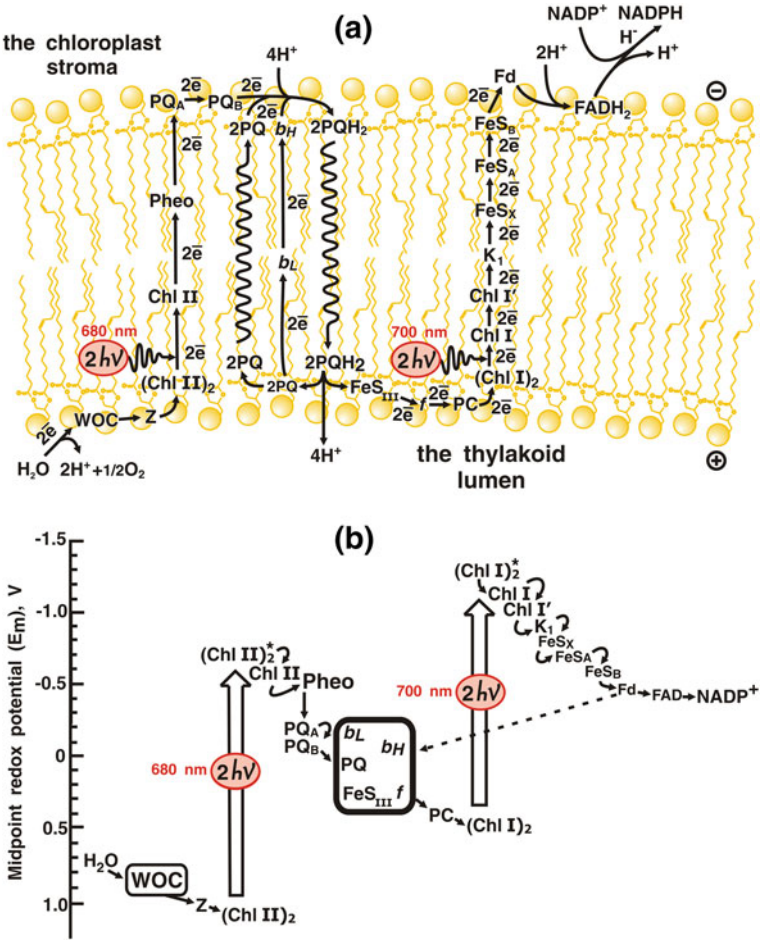

Fig. 2.21 Noncyclic light-dependent redox chain of chloroplasts (Blankenship and Prince 1985): WOC—water-oxidizing complex; *yellow*, electron-transporting prosthetic groups; Z—tyrosine residue in a protein of photosystem 2; $(ChlII)_2$—dimer of photosystem 2 chlorophyll; ChlII—monomer of photosystem 2 chlorophyll; PQ_A and PQ_B—plastoquinones bound to photosystem 2; PQ—free plastoquinone; b_H and b_L—high- and low-potential hemes of cytochrome b_6; *f*—cytochrome *f*; PC—plastocyanin; $(ChlI)_2$—dimer of photosystem 1 chlorophyll; ChlI and ChlII- monomers of photosystem 1 chlorophylls; K_I—vitamin K_1; FeS_X—primary stable electron acceptor of photosystem 1; FeS_A and FeS_B—two iron–sulfur clusters tightly bound to photosystem 1; Fd—ferredoxin. **a** Diagram illustrating the most probable arrangement of redox centers in the thylakoid membrane. **b** Reducing equivalent carriers are arranged according to their redox potentials; the dotted line shows the electron transfer pathway from ferredoxin to b_6f complex that provides cyclic electron transfer in the photoredox chain

prosthetic group. From FAD, the reducing equivalents come to $NADP^+$. The formed NADPH is oxidized by a water-soluble enzyme system reducing CO_2 to carbohydrates.

Within the framework of the scheme in Fig. 2.21, the noncyclic redox chain of chloroplasts and cyanobacteria carries out transmembrane movement of 6 H^+ per 4 quanta. This corresponds to the $H^+/\bar{e}$ ratio of 1.5 (the ratio of the number of H^+ ions transported across the membrane to the number of electrons transferred from H_2O to CO_2). *Thus, there are three* $\Delta\bar{\mu}_{H^+}$ *generators in the thylakoid redox chain—photosystem 1, photosystem 2, and the* b_6f *complex.*

2.3.2 Photosystem 1

Chloroplast photosystem 1 contains 14 different polypeptides. Two of them with molecular masses of 83.2 and 82.5 kDa show 45 % similarity (percentage of identical amino acid residues in the sequences). Other subunits are of substantially lower mass (for review see (Okamura et al. 1982; Crofts and Wraight 1983; Nelson and Ben-Shem 2004; Nelson 2011)).

$(ChlI)_2$, ChlI, ChlI′, vitamin K_1 (phylloquinone), and FeS_X are connected to large subunits, while FeS_A and FeS_B are connected to one of the small hydrophobic subunits. In contrast to photosystem 1 of cyanobacteria, four proteins carrying antenna chlorophylls (Lhca1-4) are integrated into chloroplast photosystem 1. When looking at the thylakoid membrane from the normal to the membrane plane, one will note that antenna proteins form a half-circle around the other subunits that constitute the reaction center complex of photosystem 1 (Fig. 2.22). The transfer of excitation energy from the antenna chlorophyll to $(ChlI)_2$ is extremely effective—almost every photon absorbed by the antenna leads to oxidation of $(ChlI)_2$. The copper-containing protein plastocyanin (see below), being part of photosystem 1, is located on the inner side of the thylakoid membrane, being absorbed by membrane surface. Another surface protein, ferredoxin (11 kDa), is located on its outer side. This protein contains a FeS cluster and transfers electrons from photosystem 1 to the flavoprotein that reduces $NADP^+$ (34 kDa).

The photosystem 1 reaction center complexes form trimers in the thylakoid membranes of cyanobacteria. In the case of higher plant chloroplasts, photosystem 1 is in the form of monomers. Both the trimers of cyanobacteria and the monomers of chloroplasts have been purified, crystallized, and studied by X-ray structural analysis. The results of X-ray studies of chloroplasts are shown in Figs. 2.22 and 2.23. Figure 2.23 shows two pathways of electron transfer through $(ChlI)_2^*$ to FeS_X, each containing the same redox groups (ChlI, ChlI′, and vitamin K_1). Both pathways are capable of electron transfer, but one of them is ten times faster than the other.

The primary photoprocess in photosystem 1 is the electron shift from $(ChlI)_2^*$ (redox potential −1.2 V) to ChlI (redox potential about −1 V). The electron is then transferred to ChlI′ and later to vitamin K_1 (redox potential −0.8 V). FeS_X (−0.7 V) is the next electron carrier. It is a cluster of four iron ions and four sulfide ions. In addition to this component, there are two more [4Fe − 4S] clusters (FeS_A

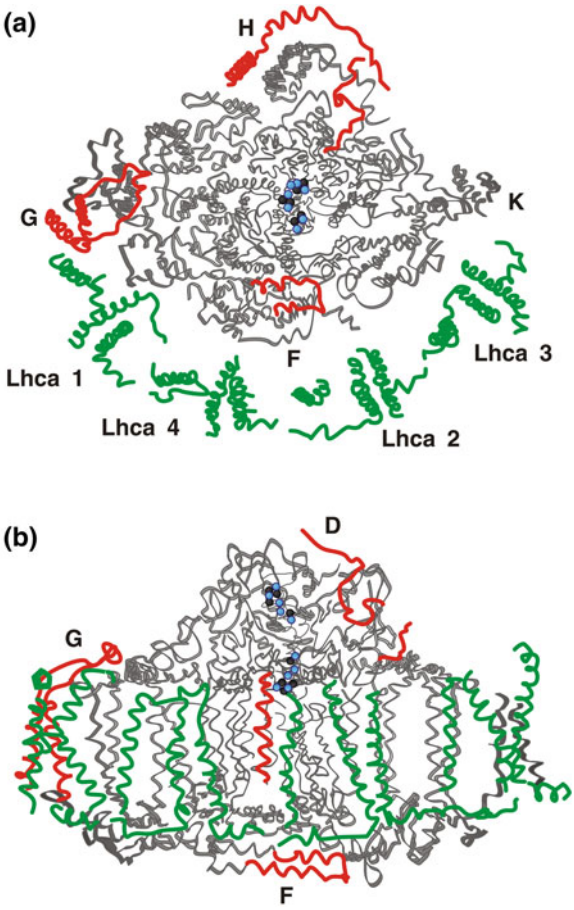

Fig. 2.22 Polypeptide body of photosystem 1 from pea chloroplasts. Four antenna proteins (Lhca 1–4) are shown in green color. Structural elements of chloroplast photosystem 1 that are different from cyanobacterial photosystem 1 are red, and those similar in chloroplasts and cyanobacteria are gray. Iron–sulfur clusters FeS_X, FeS_A, and FeS_B that all share the composition [4Fe-4S] are shown as black (Fe) and blue (S) bold dots. **a** *Top view* from chloroplast stroma side. Subunits F, G, H, and K are shown. **b** *Side view* from antenna protein side. N-terminal domains of F and D subunits that are specific for chloroplasts are in red color. X-ray analysis (Nelson and Ben-Shem 2004)

and FeS_B) in photosystem 1. Their redox potentials are −0.58 and −0.53 V, respectively. The electron transfer sequence in this segment of the redox chain is $FeS_X \rightarrow FeS_A \rightarrow FeS_B$. The latter component serves as the reductant of the water-soluble protein ferredoxin that contains a [2Fe − 2S] cluster.

Another water-soluble electron carrier is the reductant of photooxidized $(ChlI)_2^{\bullet+}$. This is plastocyanin, a copper-containing protein. The primary structure of plastocyanin has sequences homologous to those in subunit II of cytochrome oxidase, the terminal enzyme of the respiratory chain (see Sect. 4.4).

Plastocyanin is reduced by cytochrome *f*, which is a component of the b_6f complex. The latter transfers electrons from photosystem 2 to photosystem 1 (see below, Sect. 2.3.3).

There is *an alternative function of the photosynthetic redox chain in chloroplasts, namely cyclic electron transport*, with photosystem 1 and b_6f complex but not photosystem 2 being involved. This system can be demonstrated in vitro when photosystem 2 is blocked by the herbicide dichlorophenyl dimethylthiourea

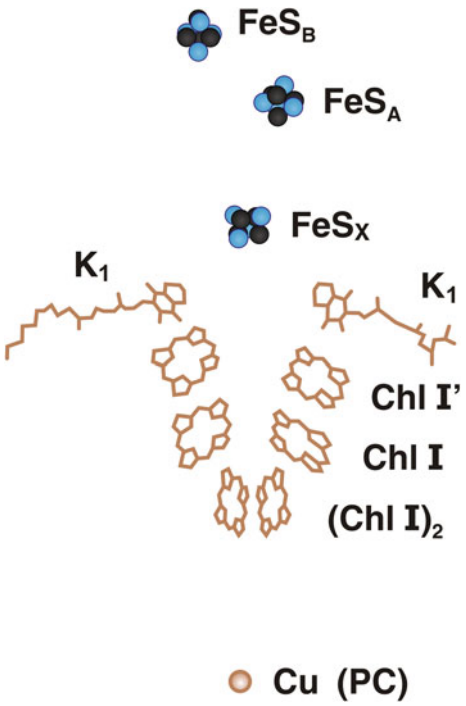

Fig. 2.23 Arrangement of prosthetic groups in chloroplast photosystem 1 on the basis of X-ray analysis (Nelson and Ben-Shem 2004)

(DCMU, also called Diuron) and an artificial electron carrier is added. Under certain natural conditions, the cyclic electron transfer seems to be operative in vivo. It has been proposed that in such case reducing equivalents are transported from ferredoxin back to $(ChlI)_2^{\bullet+}$ instead of being accepted by $NADP^+$. This process involves plastoquinone and the b_6f complex. It is suggested that ferredoxin reduces PQ, so photosystem 2 does not appear to be necessary to regenerate $(ChlI)_2$ from $(ChlI)_2^{\bullet+}$. This mechanism is similar to the cyclic redox chain of purple bacteria generating $\Delta\bar{\mu}_{H^+}$ without photolysis of water and reduction of $NADP^+$ (Crofts and Wraight 1983).

Photosystem 1 is clearly competent in generating $\Delta\bar{\mu}_{H^+}$. The reduction of Photosystem 1 by plastocyanin was shown to occur on the inner side of the thylakoid membrane, while ferredoxin and ferredoxin-$NADP^+$ reductase, which oxidize photosystem 1, are located on its outer side. Thus, the electron transport via photosystem 1 must be directed across the membrane. The photosystem 1 complex has been reconstituted into proteoliposomes, which were then found to generate $\Delta\bar{\mu}_{H^+}$ under continuous illumination. To mediate cyclic electron transfer around photosystem 1, the electron donor ascorbate and an artificial electron carrier phenazine methosulfate were added to the incubation mixture. Incorporation of a purified H^+-ATP synthase complex into the same proteoliposomes made photophosphorylation possible (Nelson and Hauska 1979; Hauska et al. 1980).

The mechanism of $\Delta\bar{\mu}_{H^+}$ generation mediated by photosystem 1 seems to be similar to that mediated by bacterial reaction centers. A nanosecond laser flash induces very fast ($\tau < 100$ ns) $\Delta\Psi$ generation, this process being much faster than any reaction in photosystem 1 other than electron transfer from $(ChlI)^*$ to FeS_X. The generated $\Delta\Psi$ composes a major part of the total electrogenesis linked with the operation of photosystem 1, so all the other stages of electron transfer make just a relatively small contribution to the energy transformation in this segment of the photosynthetic redox chain (Witt 1979; Lopez and Tien 1984).

2.3.3 Photosystem 2

Photosystem 2 was found to consist (depending on the object and purification method used) of about 30 different types of polypeptides, some of which are coded by nuclear and some by chloroplast DNA. It forms dimers. The X-ray analysis-based structure of photosystem 2 and the location of redox centers are shown in Fig. 2.24.

The photosystem 2 chlorophylls (similar to those from photosystem 1) belong to the group of a-type chlorophylls and have an α-absorption band at 680 nm (700 nm in case of photosystem 1). Subunits D1 and D2 (39.5 and 39 kDa, respectively) construct the central part of photosystem 2. These subunits resemble the M- and L-subunits of the purple bacteria reaction center complex (Hearst and Sauer 1984; Cramer et al. 1985). They bind $(ChlII)_2$, two ChlII, two pheophytins, primary and secondary quinones (PQ_A and PQ_B), nonheme iron connected to four histidines, and also two antenna chlorophylls (Chl_Z). The 39-kDa subunit specifically binds DCMU.

The presence of 12 very small subunits (3–5 kDa) is characteristic of photosystem 2. Subunits of 9.5 and 4.5 kDa form the *b*-type cytochrome with α-band maximum at 559 nm (cytochrome b_{559}). Each of the mentioned subunits contains a histidine residue with imidazole forming a coordinating bond with heme. The role of cytochrome b_{559} remains unclear. The same can be said about the *c*-type cytochrome (c_{550}), which is located on the inner (directed toward the intrathylakoid space of the thylakoid) side of the membrane. This cytochrome is present in cyanobacteria, but it is absent from chloroplasts. Cytochrome b_{559} is located closer to the opposite membrane side.

A very high redox potential of the basic state of the chlorophyll dimer (the $(ChlII)_2/(ChlII)_2^{\bullet+}$ couple) is a distinctive feature of photosystem 2 (Nelson and Ben-Shem 2004; Nelson 2011). It is equal to +1.1 V. This explains why $(ChlII)_2^{\bullet+}$ can serve as the electron acceptor for water (the redox potential of the H_2O/O_2 couple at neutral pH is + 0.82 V). On the other hand, the redox potential of the excited $(ChlII)_2^*$ is in negative (less than −0.6 V).

Plastoquinone (PQ_A) was shown to be the primary stable electron acceptor. Another bound quinone molecule (PQ_B) participates in the further electron transfer along the photosynthetic redox chain. Similar to the purple bacteria, this process is

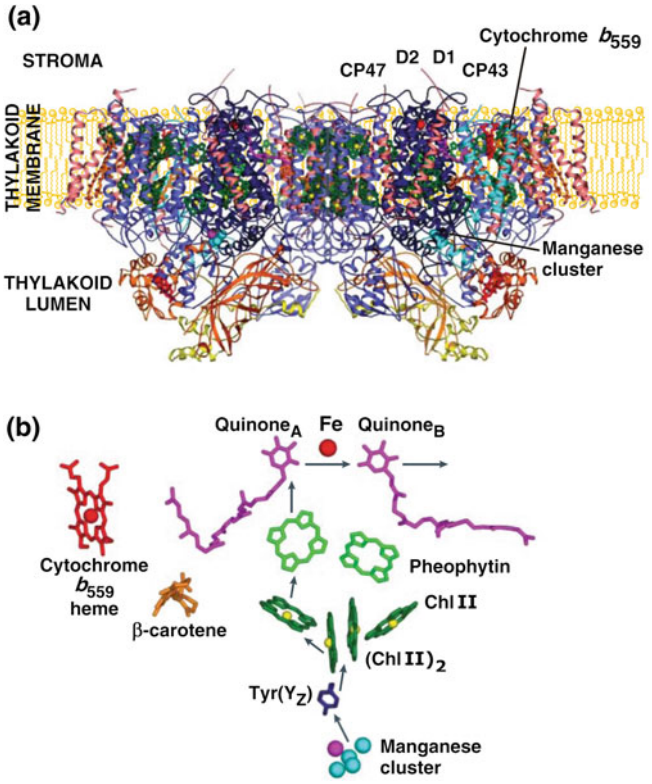

Fig. 2.24 Chloroplast photosystem 2 structure. **a** *Side view* of photosystem 2 dimer: subunits D1 and D2 are in dark blue color, chlorophyll-binding antenna proteins CP43 and CP47 are red, cytochrome b_{559} is light-blue, peripheral subunits orange and yellow, and other subunits pink. **b** spatial arrangement of photosystem 2 prosthetic groups: chlorophylls are dark green, manganese cluster light-blue, a water molecule bound to the manganese cluster pink, heme and nonheme iron red, and quinones purple. The electron transfer pathway is indicated by arrows. (Nelson and Ben-Shem 2004)

accelerated by nonheme iron, which is chelated by four histidines, and it is inhibited by *o*-phenanthroline.

A tyrosine residue of a protein acts as the primary electron donor for $(\text{ChlII})_2^{\bullet+}$. It reduces $(\text{ChlII})_2^{\bullet+}$ within 50–500 ns.

The specific *water-oxidizing complex* (WOC) is the reductant for the tyrosine radical that is formed when this amino acid residue is oxidized by $(\text{ChlII})_2^{\bullet+}$. This system operates such that a splitting of two H_2O molecules results in (i) the reduction of four $(\text{ChlII})_2^{\bullet+}$ molecules and (ii) the formation of one O_2 molecule and four H^+ ions.

The WOC is composed of four polypeptides, one of which contains four Mn^{2+} *ions* (Cramer et al. 1985). The latter participate directly in electron transfer from water to the tyrosine radical.

The mechanism of $\Delta\bar{\mu}_{H^+}$ generation by photosystem 2 can be pictured by analogy with the reaction center complex of purple bacteria that has already been discussed. Apparently, here there is also a light-dependent transmembrane movement of an electron from the excited chlorophyll dimer to Q_A located on the opposite side of the hydrophobic barrier, and only one of two ChlII- and pheophytin-containing chains is operative.

2.3.4 Cytochrome b_6f Complex

The *Q*-cycle reaction system is catalyzed by the b_6f complex in chloroplasts and cyanobacteria. This complex contains four large (18–32 kDa) and four small subunits. Three large subunits contain redox centers. These are: *cytochrome f* (32 kDa), *three-heme cytochrome* b_6 (23 kDa), and an *FeS protein* (20 kDa). The fourth large subunit (18 kDa) does not directly participate in electron transfer. The complex forms a dimer of 217 kDa. Cytochrome b_6 is unique as it contains two *b* hemes and a c_i heme (Fig. 2.25) (Stroebel et al. 2003). Both *b* hemes of cytochrome b_6 have α-maxima at 563 nm. They differ in their redox potentials. The b_L and b_H hemes have midpoint potentials (E_m) of –30 and +150 mV, respectively (Clark and Hind 1983). In chloroplast cytochrome b_6, heme c_i is covalently bound to only one cysteine, and not to two as in all other *c*-type cytochromes. The other specific feature of c_i heme is the absence of axial ligands represented by functional groups of the protein. The c_i heme is located next to the b_H heme, thus forming a kind of screen dividing it from PQ. PQ probably serves as one of the axial ligands of heme c_i. One can speculate that such a configuration of the PQ-reductase center of the b_6f complex facilitates the two-electron reduction of PQ by electrons of hemes c_i and b_H; it is also possible that this configuration reduces the lifetime of the semiquinone form of plastoquinone ($PQ^{\bullet -}$), which is dangerous due to its ability to reduce O_2 into $O_2^{\bullet -}$. The danger of such a transformation is especially high in cells with oxygenic photosynthesis, where intracellular O_2 concentration is always high.

A comparison of the amino acid sequence of cytochrome b_6 from spinach chloroplasts with those of mitochondrial cytochrome *b* from animals, plants, and fungi revealed similarity in the first 200 residues from the N-terminus. However, there is an obvious difference—cytochrome b_6 is substantially shorter (211 residues) than mitochondrial cytochromes *b* (330–385 residues). On the other hand, a considerable sequence homology was found between the fourth (18-kDa) subunit of the b_6f complex and the C-terminal part (residues 269–353) of the mitochondrial cytochrome *b*. One can assume that a function carried out by the C-terminal part of the mitochondrial cytochrome *b* is performed in the chloroplasts by the 18-kDa subunit (Widger et al. 1984; Saraste 1984).

Cytochrome b_6 contains five histidine residues, four of which participate in the coordination of the b_L and b_H hemes. These residues at positions 82, 96, 183, and 198 (197 in mitochondrial cytochrome *b*) are completely conserved, i.e. they are

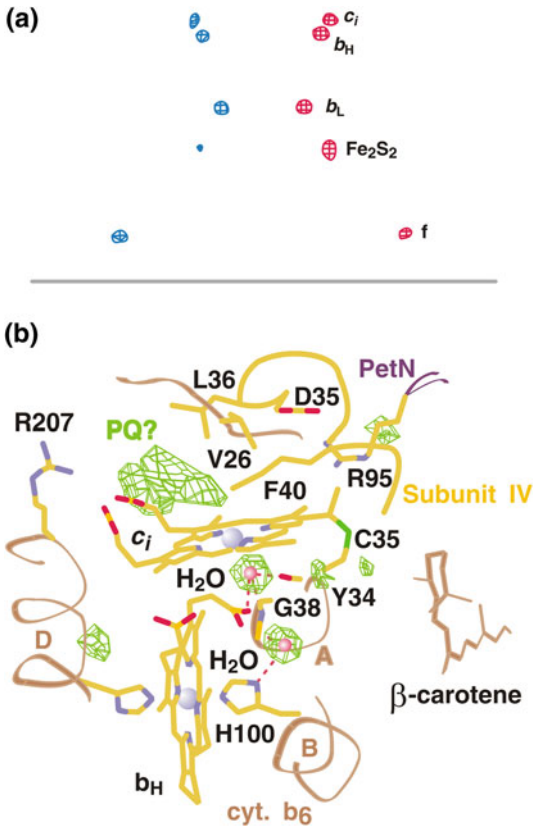

Fig. 2.25 Redox centers of the b_6f complex dimer from chloroplasts of the green alga *Chlamydomonas reinhardtii*. **a** Iron atoms of c_i, b_H and b_L hemes of cytochrome *b*, [2F-2S] cluster of FeS_{III} protein, and cytochrome *f*. **b** Surroundings of c_i and b_H hemes in cytochrome b_6. Potential axial ligand of heme c_i iron (most likely plastoquinone) and two water molecules that are bound close to c_i and b_H hemes are shown in green color (Stroebel et al. 2003)

found in cytochrome b_6 as well as in all the mitochondrial cytochromes *b* from different kingdoms of living organisms. All these histidines are always located in hydrophobic segments of the polypeptide chain. They participate in the binding of hemes b_L and b_H, thus acting as axial ligands and determining the location of the hemes perpendicular to the membrane surface. Each heme *b* contains two negatively charged propionate groups. These groups oppose conserved, positively charged arginines (Fig. 2.26) (Cramer et al. 1985).

The distance between the heme edges, according to the model, is 1.2 nm, and that between the iron atoms is 2.0 nm. This means that an electron moving from heme b_L to heme b_H needs to cross about half of the hydrophobic membrane core.

A partner of cytochrome b_6 in PQH_2 oxidation is the FeS protein of the b_6f complex that is functionally similar to the FeS_{III} component of the respiratory chain. This FeS_{III} contains two iron atoms and two sulfur atoms (Cramer et al. 1985). The next electron carrier is cytochrome *f*. The amino acid sequence of cytochrome *f* (it contains 285 residues) shows the presence of the Cys-X–Y-Cys-His sequence, which is characteristic of covalent heme binding by *c*-type cytochromes. It occurs at residues 21–25 in the N-terminal segment. His-25 and

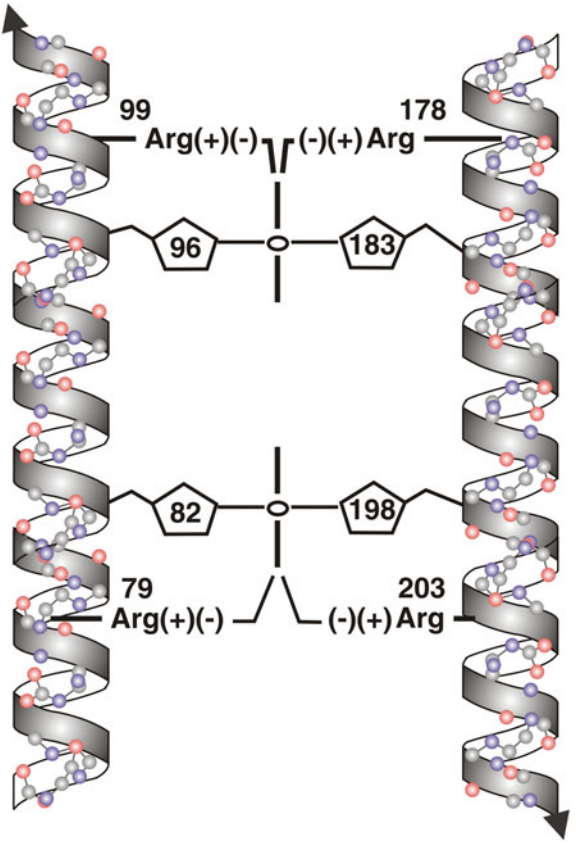

Fig. 2.26 Transmembrane arrangement of two hemes (thick vertical lines) of cytochrome b_6. Upper and lower hemes are b_L and b_H, respectively; 96, 183,83, and 198, imidazoles of corresponding histidine residues; possible stabilization of negatively charged (–) heme propionate residues by mostly conserved arginine residues (+) is shown (Cramer et al. 1985)

Lys-145 or Lys-222 serve as the ligands for the heme iron. The heme is located in the large (residues 1–250) N-terminal domain exposed to the aqueous phase in the thylakoid lumen. Residues 251–270 are hydrophobic and form an α-helical segment that functions as a membrane-spanning anchor. The remaining 15 C-terminal amino acids are located on the outer surface of the thylakoid membrane and can be removed by proteases. Segment 190–249 includes many acidic amino acid residues facing the thylakoid interior and is probably involved in interaction with a positively charged segment of cytochrome b_6. Ten conserved basic amino acids in the region 58–154 are assumed to participate in binding the next electron carrier—plastocyanin. The cytochrome *f* spectrum shows an α-band maximum at 555 nm. The redox potential of this cytochrome is +365 mV (Cramer et al. 1985).

The average diameter of the b_6f complex is about 8.5 nm. In natural membranes the complexes tend to form dimers (Cramer et al. 1985).

It should be stressed that *b_6f complex is the slowest and most vulnerable part of the photosynthetic redox chain.* The entrance to the *Q*-cycle from photosystem 2 is blocked by the potent herbicide DCMU. Certain steps of the *Q*-cycle are very

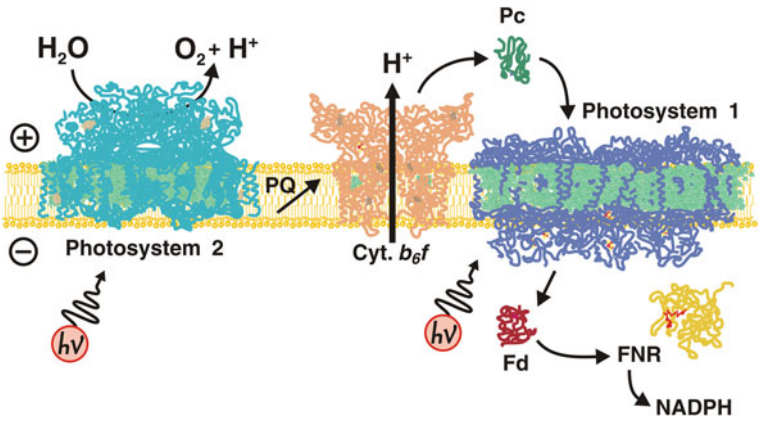

Fig. 2.27 Three $\Delta\bar{\mu}_{H^+}$ generators in the thylakoid membrane of cyanobacteria. To simplify the picture, proteins that are bound to the membrane surface, i.e. plastocyanin (PC), ferredoxin (Fd), and ferredoxin:$NADP^+$ reductase (FNR), are shown in the aqueous phases inside or outside the thylakoids

sensitive to dibromothymoquinone and 2-heptyl-4-hydroxyquinoline N-oxide. The latter two poisons are inhibitory also in mitochondrial and bacterial *Q*-cycles.

An inhibitor analysis of the thylakoid redox chain is complicated by the existence of electron transfer pathways alternative to the main noncyclic reaction sequence. This is the cyclic electron flow around photosystem 1 (and probably around photosystem 2 as well).

Figure 2.27 shows three $\Delta\bar{\mu}_{H^+}$ generators of oxygenic photosynthesis. These data were obtained by X-ray analysis of photosystem 1 and photosystem 2 and b_6f complex of cyanobacteria. The system of oxygenic photosynthesis looks very similar to the one presented in Fig. 2.27.

2.3.5 *Fate of $\Delta\bar{\mu}_{H^+}$ Generated by the Chloroplast Photosynthetic Redox Chain*

Thylakoids of chloroplasts perform only two functions—reduction of $NADP^+$ and synthesis of ATP mediated by $\Delta\bar{\mu}_{H^+}$ generation and consumption. The energy of $\Delta\bar{\mu}_{H^+}$ is quantitatively transformed into energy of ATP by the H^+-ATP synthase.

The thylakoid does not have to perform osmotic work to transport metabolites, for the aqueous intrathylakoid space is in fact enzymatically empty. The only major process that takes place on the inner surface of the thylakoid membrane is photolysis of water, resulting in formation of molecular oxygen. For both the substrate (H_2O) and product (O_2) of this reaction, crossing the membrane poses no problem. The conversion of ADP and P_i to ATP and of $NADP^+$ to NADPH both occur on the outer surface of thylakoids.

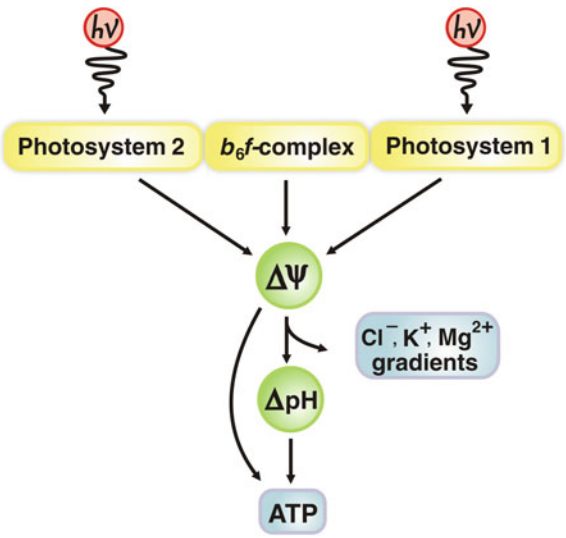

Fig. 2.28 General scheme of energy transduction in thylakoid membrane

Reverse electron transfer against the redox potential gradient is absent from thylakoids, which solve the reducing power generation problem by formation of NADPH in the noncyclic photoredox chain. Such $\Delta\bar{\mu}_{H^+}$ consumers as H^+-motors rotating bacterial flagella are also absent from thylakoids.

Since there is only one $\Delta\bar{\mu}_{H^+}$-linked function in the thylakoid membrane, there is no need to buffer $\Delta\bar{\mu}_{H^+}$ as strongly as in bacteria. Nevertheless, thylakoids have a system that can buffer $\Delta\bar{\mu}_{H^+}$ to some degree. The thylakoid membrane is rather permeable to Cl^-, K^+, and Mg^{2+}. The transport of these ions down the electric gradient formed by $\Delta\bar{\mu}_{H^+}$ generators results in the transduction of $\Delta\Psi$ to ΔpH. Since the amount of energy equivalent stored in the form of ΔpH is much larger than that in $\Delta\Psi$, the $\Delta\Psi \rightarrow \Delta pH$ transition increases the total reserve of membrane-linked energy in the system. This effect should stabilize the rate of ATP synthesis in spite of light intensity fluctuations occurring in vivo. A general scheme of energy transduction in the thylakoid membrane is shown in Fig. 2.28.

There is one more essential point that should be mentioned when discussing chloroplast energetics. It was found that H^+-ATP synthase can be absent from those parts of thylakoids in which the membranes of two adjacent thylakoids adjoin each other. This occurs when thylakoids are not swollen (i.e. have a discoid shape) and a very narrow cavity separates one thylakoid from another. In such a case, all the H^+-ATP synthase molecules were shown to be concentrated at the very periphery of the thylakoid disks exposed to the chloroplast stroma and (mainly) in membranous lamellas stretched through the stroma (see above, Fig. 2.20). These lamellas are in fact the continuation of some thylakoids. The lamellas were shown to contain mainly photosystem 1, whereas thylakoids have both photosystems. It appears that lamellas specialize in ATP synthesis coupled to cyclic electron transport around photosystem 1, and they are not capable of

photolysis of water and reduction of $NADP^+$ (these two processes occur in thylakoids). Apparently, to form ATP the thylakoid-generated $\Delta\bar{\mu}_{H^+}$ must be first transmitted along the membrane to the lamellas, where a major pool of H^+-ATP synthase is located.

When thylakoids are in a swollen state, H^+-ATP synthase molecules diffuse from the lamellas to thylakoids so as to be equally distributed between all the areas on the intrachloroplast membranes.

All the above-mentioned considerations also apply to the thylakoids of cyanobacteria, which apparently were the evolutionary precursors of chloroplasts. In this case, however, we must supplement the scheme shown in Fig. 2.27 by a respiratory chain arranged in the same thylakoid membrane. (In plant cells, the respiratory chain is located in mitochondria.) The interaction of the photosynthetic and respiratory chains that share the same components of the *Q* cycle in their middle stages will be discussed later (see Sect. 4.3.3).

References

Blankenship RE, Prince RC (1985) Excited state redox potentials and the Z scheme of photosynthesis. TIBS 10:382–383

Clark RD, Hind G (1983) Spectrally distinct cytochrome *b*-563 components in a chloroplast cytochrome *b-f* complex: Interaction with a hydroxyquinoline N-oxide. PNAS 80:6249–6253

Cramer WA, Widger WR, Herrmann RG, Trebst A (1985) Topography and function of thylakoid membrane proteins. TIBS 10:125–129

Crofts AR, Wraight CA (1983) The electrochemical domain of photosynthesis. Biochim Biophys Acta 426:149–185

Deisenhofer J, Epp O, Miki K, Huber R, Michel H (1984) X-ray structure analysis of a membrane protein complex. Electron density map at 3 Å resolution and a model of the chromophores of the photosynthetic reaction center from *Rhodopseudomonas viridis*. J Mol Biol 180:385–398

Deisenhofer J, Epp O, Miki K, Huber R, Michel H (1985a) Structure of the protein subunits in the photosynthetic reaction centre of *Rhodopseudomonas viridis* at 3Å resolution. Nature 318:618–624

Deisenhofer J, Michel H, Huber R (1985b) The structural basis of photosynthetic light reaction in bacteria. TIBS 10:243–248

Deprez J, Trissl HW, Breton J (1986) Excitation trapping and primary charge stabilization in *Rhodopseudomonas viridis* cells, measured electrically with picosecond resolution. PNAS 83:1699–1703

Drachev LA, Kaulen AD, Ostroumov SA, Skulachev VP (1974) Electrogenesis by bacteriorhodopsin incorporated in a planar phospholipid membrane. FEBS Lett 39:43–45

Drachev LA, Kaulen AD, Semenov AY, Severina II, Skulachev VP (1979) Lipid-impregnated filters as a tool for studying the electric current-generating proteins. Anal Biochem 96:250–262

Dracheva SM, Drachev LA, Zaberezhnaya SM, Konstantinov AA, Semenov A, Skulachev VP (1986) Spectral, redox and kinetic characteristics of high-potential cytochrome *c* hemes in *Rhodopseudomonas viridis* reaction center. FEBS Lett 205:41–46

Glaser EG, Crofts AR (1984) A new electrogenic step in the ubiquinol:cytochrome c_2 oxidoreductase complex of *Rhodopseudomonas sphaeroides*. Biochim Biophys Acta 766: 322–333

Hauska G, Samoray D, Orlich G, Nelson N (1980) Reconstitution of photosynthetic energy conservation. II. Photophosphorylation in liposomes containing photosystem-I reaction center and chloroplast coupling-factor complex. Eur J Biochem 111:535–543

Hauska G, Schoedl T, Remigy H, Tsiotis G (2001) The reaction center of green sulfur bacteria (1). Biochim Biophys Acta 1507:260–277

Hearst LE, Sauer K (1984) Protein sequence homologies between portions of the L and M subunit of reaction centers of *Rhodopseudomonas capsulata* and the Q_B-protein of chloroplast thylakoid membranes; a proposed relation to quinone-binding sites. Z Naturforsch 85:515–521

Henderson R (1985) Membrane proteins: structure of a bacterial photosynthetic reaction centre. Nature 318:598–599

Hu X, Damjanovic A, Ritz T, Schulten K (1998) Architecture and mechanism of the light-harvesting apparatus of purple bacteria. PNAS 95:5935–5941

Kayushin LP, Skulachev VP (1974) Bacteriorhodopsin as an electrogenic proton pump: reconstitution of bacteriorhodopsin proteoliposomes generating $\Delta\Psi$ and ΔpH. FEBS Lett 39:39–42

Krasnovsky AA (1948) Reversible photochemical reduction of chlorophylls by ascorbic acid. Dokl Akad Nauk SSSR (Russ) 60:421–424

Lopez JR, Tien HT (1984) Reconstitution of photosystem I reaction center into bilayer lipid membranes. Photobiochem Photobiophys 7:25–39

Matveetz YA, Chekalin SV, Yartsev AA (1987) Femtosecond spectroscopy of the primary photoprocesses in *Rhodopseudomonas sphaeroides* reaction centers. Dokl Akad Nauk SSSR (Russ) 292:724–728

Merchant S, Sawaya MR (2005) The light reactions: a guide to recent acquisitions for the picture gallery. Plant Cell 17:648–663

Mitchell P (1966) Chemiosmotic coupling in oxidative and photosynthetic phosphorylation. Biol Reviews 41:445–502

Mitchell P (1975) Protonmotive redox mechanism of the cytochrome bc_1 complex in the respiratory chain: protonmotive ubiquinone cycle. FEBS Lett 56:1–6

Nelson N (2011) Photosystems and global effects of oxygenic photosynthesis. Biochim Biophys Acta 1807:856–863

Nelson N, Ben-Shem A (2004) The complex architecture of oxygenic photosynthesis. Nat Rev Molec Cell Biol 5:971–982

Nelson N, Hauska G (1979) Topography, resolution and reconstitution of the chloroplast membrane Membrane Bioenergetics. Addison-Wesley, London

Okamura MY, Feher G, Nelson N (1982) Reaction centers. In: Govindjee (ed) Photosynthesis: energy conservation by plants and bacteria, vol 1. Academic Press, New York, pp 1394–1403

Parson WW (1982) Photosynthetic bacterial reaction centers: interactions among the bacterio-chlorophylls and bacteriopheophytins. Ann Rev Biophys Bioeng 11:57–80

Rich PR (1984) Electron and proton transfers through quinones and cytochrome *bc* complexes. Biochim Biophys Acta 768:53–79

Robert B, Lutz M, Tiede DM (1985) Selective photochemical reduction of either of the two bacteriopheophytins in reaction centers of *Rps. sphaeroides.* FEBS Lett 183:326–330

Saraste M (1984) Location of haem-binding sites in the mitochondrial cytochrome *b*. FEBS Lett 166:367–372

Severina II (1982) Nystatin: induced increase in photocurrent in the system "bacteriorhodopsin proteliposome/bilayer planar membrane". Biochim Biophys Acta 681:311–317

Shuvalov VA, Asadov AA (1979) Arrangement and interaction of pigment molecules in reaction centers of *Rhodopseudomonas viridis*. Photodichroism and circular dichroism of reaction centers at 100 K. Biochim Biophys Acta 545:296–308

Shuvalov VA, Duysens LN (1986) Primary electron transfer reactions in modified reaction centers from *Rhodopseudomonas sphaeroides*. PNAS 83:1690–1694

Shuvalov VA, Amesz J, Duysen LNM (1986) Picosecond charge separation upon selective excitation of the primary electron donor in reaction centers of *Phodopseudomonas viridis*. Biochim Biophys Acta 851:327–330

Skulachev VP (1972) The driving forces and mechanisms of ion transport through coupling membranes. FEBS Simposia 28:371–385

Skulachev VP (1988) Membrane bioenergetics. Springer, Berlin

Stroebel D, Choquet Y, Popot JL, Picot D (2003) An atypical haem in the cytochrome b_6f complex. Nature 426:413–418

Wakao N, Yokoi N, Isoyama N, Hiraishi A, Shimada K, Kobayashi M, Kise H, Iwaki M, Itoh S, Takaichi S, Sakurai Y (1996) Discovery of natural photosynthesis using Zn-containing bacteriochlorophyll in an aerobic bacterium *Acidiphilium rubrum*. Plant Cell Physiol 37:889–893

Widger WR, Cramer WA, Herrmann RG, Trebst A (1984) Sequence homology and structural similarity between cytochrome *b* of mitochondrial complex III and the chloroplast b_6f complex: position of the cytochrome *b* hemes in the membrane. PNAS 81:674–678

Witt HT (1979) Energy conversion in the functional membrane of photosynthesis. The central role of the electric field. Biochim Biophys Acta 505:335–427

http://www.springer.com/978-3-642-33429-0

Principles of Bioenergetics

Skulachev, V.; Bogachev, A.V.; Kasparinsky, F.O.

2013, XVI, 436 p., Hardcover
ISBN: 978-3-642-33429-0